Supplementary Materials

Develop Two-Dimensional, Highly Mass-Transferred Solid Superacids with Extremely-High Acid Strength and Superior Catalytic Performance

Fujian Liu*,[1,2] Xianfeng Yi[3], Wei Chen[3,4], Zhiqiang Liu[3,4], Wei Chen[5], Chen-Ze Qi,[1] Yu-Fei Song[5], Anmin Zheng*[3]

[1] Key Laboratory of Alternative Technologies for Fine Chemicals Process of Zhejiang Province, College of Chemistry and Chemical Engineering, Shaoxing University, Shaoxing, 312000, China. E-mail: fjliu@fzu.edu.cn

[2] National Engineering Research Centre of Chemical Fertilizer Catalyst (NERC-CFC), School of Chemical Engineering, Fuzhou University, Fuzhou, 350002, China. E-mail: fjliu@fzu.edu.cn

[3] Wuhan Center for Magnetic Resonance, Key Laboratory of Magnetic Resonance in Biological Systems, State Key Laboratory of Magnetic Resonance and Atomic and Molecular Physics, Wuhan Institute of Physics and Mathematics, Chinese Academy of Sciences, Wuhan 430071, China. E-mail: zhenganm@wipm.ac.cn

[4] University of Chinese Academy of Sciences, Beijing 100049, China.

[5] State Key Laboratory of Chemical Resource Engineering, Beijing University of Chemical Technology, 100029 Beijing, China.

Experimental Procedures

Chemicals and regents

All reagents were of analytical grade and used as purchased without further purification. Amberlyst-15, $H_3O_{40}PW_{12}$, 5-hydroxymethylfurfural (HMF) 1-n-butyl-3-methylimidazolium ([C_4mim]Cl), tripalmitin, crystalline cellulose of Avicel were purchased from Sigma-Aldrich Co., Ltd (USA). Montmorillonite K10 (MMT), aniline, pyrrole, CH_2Cl_2, H_2SO_4, HSO_3CF_3, HCl, ammonium persulphate, 1,3-propanesultone, ethanol, methanol, n-dodecane, and sunflower oil were purchased from Sinopharm Chemical Reagent Co., Ltd, Shanghai, China. H-USY was supplied by Sinopec Catalyst Co.

Synthesis of 2D hybrid solid acids

Synthesis of 2D MMT@polymer nanocomposites

MMT@polymer nanocomposites of MMT@PAN and MMT@PPY were synthesized from intercalation of aniline and pyrrole monomers into the internal layer of MMT *via* ion exchanging, followed by polymerization of the introduced monomers to give MMT@PAN and MMT@PPY composites. Typically, 0.6 g of aniline and pyrrole was dispersed into 40 mL of water, and the pH value of the mixture was adjusted to 2.0~3.0 by using HCl. Then, 2.0 g of MMT was introduced into the mixture, and ion exchanging was lasted for 24 h under vigorous stirring. After that, an aqueous solution containing 1.04 g of ammonium persulphate initiator and 15 mL of water was slowly introduced into the mixture. The polymerization process was lasted for 24 h at room temperature under vigorous stirring to give MMT@PAN and MMT@PPY nanocomposites. MMT@PAN and MMT@PPY could be collected from filtration, washed with abundant water until neutral, and dried at 80 °C under vacuum condition. To get MMT@PAN and MMT@PPY with different amount of polymer additives, 0.2, 0.4 and 0.8 g of aniline or pyrrole were used at the initial step, which give the samples of MMT@PAN/PPY-0.2, MMT@PAN/PPY-0.4 and MMT@PAN/PPY-0.8.

Sulfonation of 2D MMT@polymer nanocomposites

The 2D hybrid solid acids were synthesized from acidification of MMT@PAN and MMT@PPY, which was achieved from quaternary ammonization of MMT@PAN and MMT@PPY with 1,3-propanesultone, and anion-exchange with strong acids of H_2SO_4 or HSO_3CF_3. Typically, 1.0 g of MMT@PAN or MMT@PPY was dispersed into 30 mL of toluene, followed by addition of 0.5 g of 1,3-propanesultone. The reaction temperature was quickly increased up to 100 °C, and the reaction was lasted for 12 h under vigorous stirring. The sample could be collected from filtration, washed with large amount of CH_2Cl_2, dried at 80 °C under vacuum condition, which give MMT@PAN-$[C_3N]^+$ and MMT@PPY-$[C_3N]^+$ intermediates. Finally, the sample was anion-exchanged with strong acids of H_2SO_4 or HSO_3CF_3 as the following procedures: 1.0 g of MMT@PAN-$[C_3N]^+$ was added into the mixture containing 20 mL of toluene and 3.5 mL of HSO_3CF_3, after stirring of the mixture at room temperature for 48 h, the sample donated as MMT@PAN-[C_3N][SO_3CF_3] was obtained, which could be collected from filtration, washed with abundant CH_2Cl_2, and dried at 80 °C under vacuum condition. The anion-exchanging process was repeated for two times. Finally, the ion-exchanged samples were washed with abundant mixture solvent of ethanol and dichloroethane for removal of any physically adsorbed CF_3SO_3H due to their very good solubility in ethanol. Meanwhile, MMT@PAN-[C_3N][SO_4H] and MMT@PPY-[C_3N][SO_4H] could also be synthesized with similar procedure, where H_2SO_4 was used in the exchanging process. For comparison, their homogeneous counterpart of PAN/PPY-[C_3N][SO_4H] could be synthesized from directly sulfonation of PAN/PPY with similar procedures. Similarly, MMT@PAN-[C_3N][SO_4H]-0.2 and MMT@PAN-[C_3N][SO_4H]-0.4 and MMT@PAN-[C_3N][SO_4H]-0.8 could also be synthesized from sulfonation of MMT@PAN-0.2, MMT@PAN-0.4 and MMT@PAN-0.8 nanocomposites.

For comparison, PAN-[C_3N][SO_3CF_3] could also be intercalated into graphitic oxide (GO) with similar procedures as that of MMT@PAN-[C_3N][SO_3CF_3], and GO was used as the scaffold instead of MMT. GO was synthesized by using Hummers method as described previously.[S1] SBA-15-SO_3H-0.2 with molar ratio of S/Si at 0.2 and porous SO_4^{2-}/ZrO_2 solid acids were synthesized according to the literature.[S2,S3]

Preparation of MMT@carbon and MMT-carbon

For comparison, the PAN-[C_3N][SO_3CF_3] wrapped MMT was synthesized by skipping the ion exchanging process. The ion exchanging process plays key factor for insertion of aniline monomer into the interlayer of MMT. In the sample's preparation, 0.6 g of aniline was dispersed into 40 mL of water, and the pH value of the mixture was adjusted to 2.0~3.0 by using HCl. Then, 2.0 g of MMT together with 15 mL of ammonium persulphate (~1.04 g) aqueous solution were introduced into the mixture. The polymerization process was lasted for 12-24 h at room temperature under vigorous stirring and the product was collected by filtration and washed by water until neutral, dried at 80 °C under vacuum condition. The polymer-wrapped MMT sample was denoted as MMT-PAN. MMT-PAN was then quaternary ammonized with 1,3-propanesultone, and anion-exchanged with HSO_3CF_3 to give PAN-$[C_3N][SO_3CF_3]$ wrapped MMT (MMT-PAN-$[C_3N][SO_3CF_3]$). The MMT-PAN-$[C_3N][SO_3CF_3]$ and MMT@PAN-$[C_3N][SO_3CF_3]$ samples were carbonized at 600 °C for 2h under vacuum condition, and treated with HF (25wt%) to remove MMT scaffold, then MMT-Carbon and MMT@Carbon were obtained.

Characterizations

X-ray powder diffraction (XRD) of the samples was recorded on a Rigaku D/max2550 PC powder diffractometer with Cu-Kα radiation ($\lambda = 0.15406$ nm) in the range of $4° \leq 2\theta \leq 30°$. Nitrogen adsorption-desorption isotherms were measured using a Micromeritics ASAP 2020M system. The samples were outgassed for 10 h at 150 °C before the measurements. The pore-size distribution for mesopores was calculated using Barrett-Joyner-Halenda (BJH) model. FT-IR spectra were recorded by using a Bruker 66V FT-IR spectrometer. Thermogravimetric analysis (TG) was performed on a Perkin-Elmer TGA7 and a DTA-1700 in flowing air, respectively. The heating rate was 10 °C/min. Scanning electron microscopy (SEM) images were taken on Hitachi 4800 with the acceleration voltage of 5 kV. Transmission electron microscopy (TEM) images were taken on a Hitachi HT7700 transmission electron microscope. The high-resolution TEM, HAADF-STEM images, and the corresponding energy-dispersive X-ray (EDX) mapping were recorded by a JEOL JEM-2100F high resolution transmission electron microscope with the acceleration voltage of 200 kV. Contact angles were tested on DSA10MK2G140, Kruss Company, Germany. XPS spectra were performed on a Thermo ESCALAB 250 with Al Kα radiation at y=901 for the X-ray sources, the binding energies were calibrated using the C1s peak at 284.9 eV. The molecular weight of the intercalated PAN-$[C_3N][SO_3CF_3]$ and PPY-$[C_3N][SO_4H]$ were measured by gel permeation chromatography (Waters 1525), using a RI detector (1424). Before the test, PAN-$[C_3N][SO_3CF_3]$ and PPY-$[C_3N][SO_4H]$ have to be obtained from the treatment of MMT@PAN-$[C_3N][SO_3CF_3]$ and MMT@PPY-$[C_3N][SO_4H]$ with HF to remove MMT scaffold. The intercalated PAN-$[C_3N][SO_3CF_3]$ and PPY-$[C_3N][SO_4H]$ in MMT can not be removed by extracted with various kinds of solvents such as DMF, THF and $CHCl_3$ due to their very strong interactions with MMT scaffold. The PAN-$[C_3N][SO_3CF_3]$ and PPY-$[C_3N][SO_4H]$ were dissolved in dimethylformamide (DMF), which was also used as the mobile phase (flow rate, 1.0 mL/min). The injection volume was 10 μL, and the column temperature was maintained at 35 °C. Polystyrene was used as standard.

^{31}P solid state NMR spectra

All the NMR experiments were performed on a Bruker AVANCE-III 500 MHz spectrometer at Larmor frequencies of 500.57, and 202.63 MHz for ^{1}H, and ^{31}P nucleus, respectively, with a 4 mm magic-angle-spinning (MAS) probe operating at a spinning rate of 12 kHz. A single-pulse sequence with a $\pi/2$ pulse length of 4.0 μs and a recycle delay of 5 s was used for the ^{1}H NMR experiments. ^{31}P MAS NMR spectra with high power proton decoupling were recorded using a $\pi/2$ pulse length of 3.3 μs and a recycle delay of 15 s. The chemical shifts of ^{1}H, and ^{31}P nucleus were externally referenced to adamantane, and $(NH_4)_2HPO_4$ (1 ppm), respectively. Prior to the NMR experiments, the synthesized 2D hybrid solid acids were performed as follows: before the sorption of probe molecules, the sample was placed into a glass tube and then connected to a vacuum line for dehydration at 180 °C. The temperature was gradually increased to 180 °C with a heating rate of 1 °C/min, and the system pressure was kept below 10^{-3} Pa over a period of 10 h and then cooled down to room temperature. Subsequently, sufficient volatile TMP molecule was transfer onto the sample frozen over a liquid N_2 bath. Then, the sample was evacuated at room temperature for 1 h to remove physisorbed TMP molecules after the adsorption was equilibrated. Finally, the sample tube was flame-sealed. The detailed procedures involved in introduction of TMPO probe molecule onto the sample can also be found elsewhere.[S4–S6] In brief, a certain amount of TMPO adsorbate dissolved in anhydrous CH_2Cl_2 was firstly added into a vessel containing the dehydrated sample in a N_2 glove box, then the CH_2Cl_2

solvent was removed from evacuation at room temperature. To ensure a uniform adsorption of adsorbate probe molecules in the pores/channels of the synthesized 2D solid acids, the sealed sample vessel was further subjected to a thermal treatment at 160 °C for 2 h. Prior to NMR measurements, the sealed sample tube was opened and the sample was transferred into a NMR rotor with a Kel-F end cap under a dry nitrogen atmosphere in a glove box. A single-pulse sequence with a π/2 pulse length of 4.0 μs and a recycle delay of 5 s was used for the ^1H NMR experiments. It is noteworthy that ca. 5000 accumulations were used for testing MMT scaffold for its relative low acidic concentration, while only 256 accumulations were employed for MMT@PAN-[C_3N][SO_3CF_3].

Potentiometric titration characterization

The Hammett indicator solution (~0.5 *wt*%) was prepared in an inert atmosphere condition, which could be obtained by dissolving Hammett indicators in benzene. Then, 5 mL of resultant Hammett indicator solution was contacted with 20 mg of MMT@PAN-[C_3N][SO_3CF_3] in a 25 mL of glassware. The resultant suspension was stirred at 30 °C for 6 h, and then color changes of indicator solution were recorded (Figure S14). The potentiometric titration was also performed to confirm the superacidity of MMT@PAN-[C_3N][SO_3CF_3], which prevents color interference of the dark sample. 20 mg of sample was dispersed into 50 mL of acetonitrile solvent, after stirring of the mixture for 6 h at room temperature, the initial electric potential was recorded. Then, 0.05 N n-butylamine was used as the titrant, the consumed volume of n-butylamine and titration curves were recorded.

Treating of MMT@PAN-[C_3N][SO_3CF_3] with trifluoroacetic acid

To breakdown the hydrogen bonding interaction between intercalated PAN-[C_3N][SO_3CF_3] and MMT, MMT@PAN-[C_3N][SO_3CF_3] was treated with trifluoroacetic acid as the literature.[S7] Typically, 0.5 g of MMT@PAN-[C_3N][SO_3CF_3] was dispersed into 10 mL of trifluoroacetic acid, after stirring of the mixture for 24 h at room temperature, the treated MMT@PAN-[C_3N][SO_3CF_3] could be collected from filtration, washing with abundant CCl_4 for removing the residual trifluoroacetic acid, and drying at 60 °C under vacuum condition.

Theoretical calculation

To better understand the prolonging of O-H bond in the sulfonate group in 2D solid acid, a series of theoretical calculations were preformed, and the sulfonated aniline and pyrrole monomer ions were used to represent their corresponding polymers (PAN-[C_3N][SO_4H] and PPY-[C_3N][SO_4H]) for model simplification and computational cost saving. The geometry optimization of ions in MMT and gas phase were performed by the GGA functional, with formulas of Perdew, Burke, and Ernzerhof (PBE) functional[S8] with Double Numerical plus Polarization (DNP) basis set on the DMol^3 code[S9,S10] and Grimme's DFT-D[S11] was considered to preferably deal with the dispersion interaction. During the optimization, the bottom layer of Si and O atoms was fixed to keep the regular structure. The visualization of calculated results was used by VESTA program.[S12]

Catalytic reactions

Esterification of acetic acid with cyclohexanol

0.15 g of catalyst and 11.5 mL (0.11 mol) of cyclohexanol were mixed well in a three-necked round flask equipped with a condenser and a magnetic stirrer. After heating of the mixture to 100 °C by oil bath, 17.5 mL (0.305 mol) of acetic acid was rapidly added and the reaction was continued for 5 h. In this reaction, the stirring rate was kept at 0, 300, 600 and 1000 rpm, the molar ratio of acetic/cyclohexanol acid was 2.6 and the mass ratio of catalyst/cyclohexanol was 0.0136. For comparison, H_2SO_4 was also used to catalyze esterification of acetic acid with cyclohexanol, where the same number of acid site (H^+) with that of MMT@PAN-$[C_3N][SO_3CF_3]$ was used in this reaction.

Transesterification of plant oil into biodiesel

Transesterification of tripalmitin with methanol was performed as following procedure: 0.84 g (1.04 mmol) of tripalmitin melted into a three-necked round flask equipped with a condenser and a magnetic stirrer at 65 °C, followed by addition of 3.76 mL of methanol and 0.075 g of catalyst, the reaction was continued for 14 h at 65 °C. In this reaction, the molar ratio of tripalmitin/methanol was nearly 1/90 and the mass ratio of catalyst/tripalmitin was 0.0595.

Transesterification of low quality plant oil with methanol was performed as the following procedure: 1.0 g of sunflower oil (1.16 mmol) and 0.15 g of catalyst were added into a three-necked round flask equipped with a condenser and a magnetic stirrer, and the reaction temperature was rapidly increased to 80 °C. Then, 3.5 mL of methanol (86.3 mmol) was quickly introduced under vigorous stirring, the reaction was lasted for 18 h. The molar ratio of sunflower oil/methanol was 1/72.1 and the mass ratio of catalyst/sunflower oil was 0.15. The main products in this reaction were methyl palmitate ($C_{16:0}$), methyl stearate ($C_{18:1}$), methyl oleate ($C_{18:2}$), methyl linoleate ($C_{18:3}$), methyl arachidate ($C_{20:0}$), 11-eicosenoic methyl ($C_{20:1}$), methyldocosanoate ($C_{22:0}$) and methyltetracosanoate ($C_{24:0}$). The quantitative analysis of these products was performed on an Agilent GC/MS instrument (Agilent 6890N/5975I) equipped with a programmable split/splitless injector. The injector-port temperature was set at 270 °C. The oven-temperature program was initially set at 140 °C and ramped to 270 °C with the ramping rate of 10 °C min^{-1}. The sample could be easily recovered from filtration, washed with abundant methanol and drying at 60 °C for 12 h under vacuum condition. Before recycling, the catalyst was activated with H_2SO_4 or HSO_3CF_3 in the CH_2Cl_2 system for 12 h, washing with abundant CH_2Cl_2 for removing absorbed H_2SO_4 or HSO_3CF_3, and drying at 60 °C for 12 h under vacuum condition, which was used directly for the next time.

In the reactions of transesterification, all of the products were analyzed by gas chromatography of Agilent 7890 with a flame ionization detector (FID). The column was HP-INNOWax capillary column (30 m); the initial temperature was 100 °C, ramping rate was 20 °C/min, and final temperature was 280 °C; the temperature of FID detector was 350 °C. In these reactions, dodecane was used as an internal standard.

Depolymerization of crystalline cellulose

Preparation of DNS Reagent

As a typical run for preparation of DNS solution, 182 g of potassium sodium tartrate was added into 500 mL of hot deionized water at 50 °C, followed by addition of 6.3 g of 3,5-dinitrosalicylic acid (DNS) and 262.0 mL of 2.0 M NaOH, after dissolved, 5.0 g of phenol and 5.0 g of sodium sulfite were also introduced into the solution under vigorous stirring, after homogeneous solution was formed, the hot solution was cooled to room temperature and diluted with deionized water to 1000 mL to give the DNS reagent.

Reaction processes

As a typical run, 100.0 mg of crystalline cellulose of Avicel was dissolved into 2.0 g of $[C_4mim]Cl$ ionic liquid at 100 °C for 1 h under stirring condition until a clear solution was formed. Then, 20.0 mg of MMT@PAN-$[C_3N][SO_3CF_3]$ was added, further stirring for 5 min to result in good dispersion of catalyst in reaction mixture, followed by addition of 600 μL of water. At different time intervals, samples were withdrawn, weighed, quenched immediately with cold water, and centrifuged at 14,800 rpm for 5 min for removing of catalysts and unreacted cellulose, giving the reaction mixture, which were collected and stored at 0 °C before DNS assay and HPLC analysis. In the meanwhile, the isolated cellulose was thoroughly washed with water, and recovered by centrifugation. The amount of cellulose isolated was determined by weighing.

Testing Total Reducing Sugar (TRS)

TRS were tested through DNS method.[S13,S14] As a typical run, a mixture containing of 0.5 mL of DNS regent and 0.5 mL of performed reaction mixture was heated for 5 min at 100 °C, after cooled to room temperature, 4 mL of deionized water was added for diluting the mixture. The color intensity of the mixture was measured in a NanoDrop 2000 UV-spectrophotometer at 540 nm. The concentration of total reducing sugars was calculated based on a standard curve obtained with glucose.

The concentrations of glucose and cellobiose in the reaction mixture were measured by HPLC system, in a Water 717plus autosampler (USA) system, in a Aminex HPX-87H column and with a refraction index detector. The column's temperature was set to 65 °C. The volume of the injection was 10 µL. The eluent consisted of a previously filtered and degasified solution of sulfuric acid 5 mM at a flow of 0.5 (mL/min).

Adsorption of Avicel by 2D solid acid of MMT@PAN-[C_3N][SO_4H]

As a typical run, 100 mg of crystalline cellulose of Avicel was dissolved into 2.0 g of [C_4mim]Cl ionic liquid at 100 °C for 1 h under stirring condition until a clear solution was formed. Then, 100 mg of MMT@PAN-[C_3N][SO_4H] was added, after stirring of the mixture at 100 °C for 2 h until the adsorption achieves equilibrium. The MMT@PAN-[C_3N][SO_4H] could be separated from centrifugation at 14,800 rpm for 10 min, washed with abundant ether and dried at 100 °C for 12 h under vacuum condition. The resultant MMT@PAN-[C_3N][SO_4H]-Avicel composite was then characterized by N_2 adsorption-desorption isotherm.

Table S1 Structural parameters and acid concentrations of various samples.

Samples	S contents (mmol/g) [a]	H^+ contents (mmol/g) [b]	S_{BET} (m^2/g) [c]	Pore diameter (nm) [c]	V_p (cm^3/g) [c]
MMT	-	-	101	5.7&24.1&129.2	0.179
MMT@PAN	-	-	97	2.5&28.2&123.4	0.092
MMT@PPY	-	-	78	2.3&29.2&126.1	0.089
MMT@PAN-[C_3N][SO_4H]	1.30	1.71	54	3.2&31.2&123.7	0.084
MMT@PPY-[C_3N][SO_4H]	1.36	1.83	29	3.1&29.1&120.5	0.076
MMT@PAN-[C_3N][SO_3CF_3]	1.24	1.32	37	8.9&23.7&126.2	0.083
MMT@PAN-[C_3N][SO_3CF_3] [d]	1.22	1.27	33	9.2&23.1&128.3	0.081
Amberlyst-15	4.30	4.70	45	40	0.31
Nafion NR50	-	0.82	-	-	-

PAN-[C_3N][SO_4H]	3.74	3.89	-	-	-

[a] Measured by CHNS elemental analysis. [b] Measured by acid-base titration. [c] Measured by N_2 adsorption-desorption isotherms. [d] The sample has been recycled for 5 times in transesterification of sunflower oil with methanol.

Table S2 TOFs values of various acid catalysts in esterification and transesterification at different reaction temperatures.

Samples	Esterification of acetic acid with cyclohexanol (TOF, h^{-1}) [a]				Transesterification of tripalmitin with methanol (TOF, h^{-1}) [b]			
	60 °C	80 °C	100 °C	120 °C	45 °C	55 °C	65 °C	75 °C
MMT@PAN-[C_3N][SO_3CF_3]	9399	26324	41382	125032	32.2	38.8	41.2	48.7
Amberlyst-15	338	1142	3455	9506	4.9	6.4	8.3	9.9
H_2SO_4	3870	9649	13558	27354	3.1	7.3	10.8	13.2
Nafion NR50	1076	4408	9820	16709	7.4	8.2	9.6	10.5

[a] 1.15 mL of cyclohexanol, 2.0 mL of acetic acid, 0.015 g catalyst, the reaction was continued for 10 min at 60, 80, 100, and 120 °C, respectively.

[b] 0.84 g (1.04 mmol) of tripalmitin, 5.0 mL of methanol and 0.075 g of catalyst, the reaction was continued for 3 h at 45, 55, 65, and 75 °C, respectively.

Table S3 Pore size and diffusion coefficient (*D*) of methanol and acetic molecules in montmorillonite (MMT) and zeolites [a].

	Pore Size (Å)	D_{Methanol} 10^{-10} m^2/s	MMT / Framework	$D_{\text{Acetic acid}}$ 10^{-10} m^2/s	MMT / Framework
MMT	13.3	857.1	1	320.2	1
MFI	5.3	10.4	82	0.38	881
MOR	6.5	14.3	60	11.9	27
VFI	12.7	80.1	11	33.3	10

[a] Estimated from molecular dynamics simulation.

Table S4 Comparison of initial reaction rates, conversions and TOFs values of various acid catalysts in transesterification of tripalmitin with methanol.

Samples	Temperature (˚C)	Conversion (%)	Rate (mmol/g·s)	TOF (h^{-1})
MMT@PAN-[C_3N][SO_3CF_3]	55	3.24	0.037	101.9
	60	4.01	0.046	126.4
	65	4.52	0.052	142.2
	70	6.04	0.071	194.0
H_2SO_4	55	2.68	0.031	5.5
	60	3.99	0.046	8.1
	65	4.14	0.048	8.5
	70	5.98	0.069	12.2

$H_3PW_{12}O_{40}$	55	2.44	0.028	97.5
	60	3.43	0.040	137.2
	65	4.04	0.047	161.7
	70	4.25	0.049	170.0
Nafion NR50	55	1.15	0.013	58.4
	60	1.49	0.017	75.9
	65	1.59	0.018	80.9
	70	1.88	0.022	95.8
Amberlyst-15	55	0.48	0.006	4.2
	60	2.09	0.024	18.5
	65	2.17	0.025	19.2

	70	2.82	0.033	24.9
SBA-15-SO_3H-0.2	55	2.47	0.028	39.4
	60	2.77	0.032	44.3
	65	2.93	0.034	46.9
	70	3.18	0.037	50.9

Reaction condition: 0.84 g (1.04 mmol) of tripalmitin, 3.76 mL of methanol, 0.075 g of catalyst, the reaction was continued for 0.5 h^{-1} at 55, 60, 65 and 70 °C, respectively.

Table S5 Catalytic data in transesterification of sunflower oil with methanol over various acid catalysts [a].

Catalysts	Yields of methyl esters (%)							
	Methyl palmitate ($C_{16:0}$)	Methyl stearate ($C_{18:1}$)	Methyl oleate ($C_{18:2}$)	Methyl linoleate ($C_{18:3}$)	Methyl arachidate ($C_{20:0}$)	Methyl 11-eicosenoate ($C_{20:1}$)	Methyldocosanoate ($C_{22:0}$)	Methyltetracosanoate ($C_{24:0}$)
MMT@PAN-[C_3N][SO_3CF_3]	97.8	98.5	99.1	98.4	97.9	97.8	97.5	98.1
MMT@PAN-[C_3N][SO_4H]	96.3	97.2	98.3	96.4	97.1	96.5	96.1	96.9
MMT@PAN-[C_3N][SO_4H]-0.4	95.1	96.7	96.3	94.2	94.5	96.3	95.4	95.4
MMT@PPY-[C_3N][SO_4H]	96.5	96.9	97.8	97.2	96.7	96.8	95.7	96.8
MMT@PAN-[C_3N][SO_4H] [b]	97.1	97.3	98.1	96.6	96.1	95.9	95.8	96.4
H_2SO_4 [c]	96.1	96.8	98.1	97.2	96.5	96.6	95.9	96.8
PAN-[C_3N][SO_4H]	86.5	87.2	86.9	89.2	87.1	88.3	87.5	89.1

SO_4/ZrO_2 [d]	40.9	38.7	36.8	40.5	29.3	33.8	34.6	37.9
$H_3PW_{12}O_{40}$	73.6	72.1	72.5	73.4	70.1	69.8	73.4	74.1
SBA-15-SO_3H-0.2 [e]	56.3	58.2	54.5	54.7	45.2	33.5	40.8	40.7
Amberlyst-15	51.7	49.2	43.2	46.8	31.1	30.6	36.6	29.8
H-USY [f]	18.5	14.6	20.6	16.1	14.2	11.2	12.9	9.3

[a] 1.0 g of sunflower oil (1.16 mmol), 2.5 mL of methanol (61.9 mmol), 0.1 g of catalyst, reaction temperature 80 °C, reaction time 18 h. The catalytic activity of the catalyst was characterized quantitatively by the conversion of fatty acid methyl esters (FAME, Y%), which was calculated as follows: Yield=(M_D/M_T)×100%, where M_D and M_T are the number of moles of each FAME produced and expected, respectively. In this section, M_T is the number of moles of FAME catalyzed by 0.15 g of H_2SO_4 at 80 °C for 24 h, and the same content of feedstock as that of other solid acids was employed. [b] The sample has been recycled for five times. [c] The same number of acid site as that of MMT@PAN-[C_3N][SO_3CF_3]. [d,e] Synthesized from ref. S2, S3. [f] Supplied by Sinopec Catalyst Co.

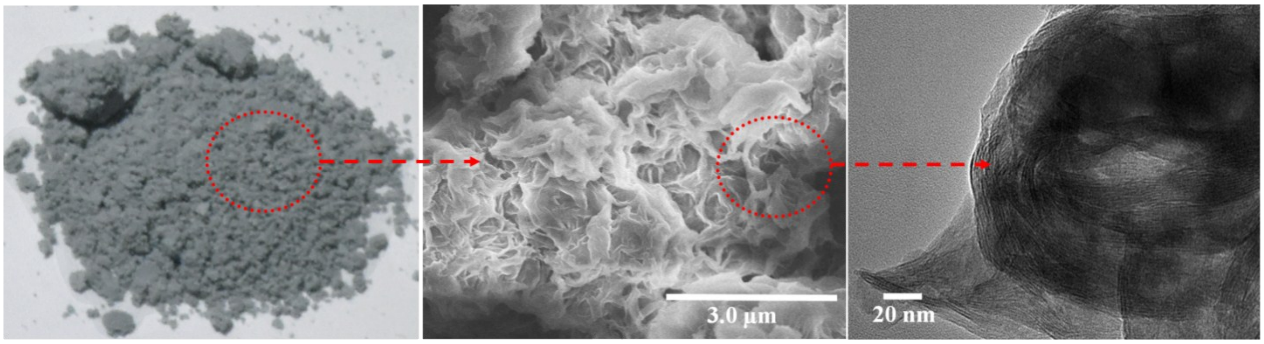

Figure S1 Morphology and micro-nano structures of MMT@PAN-[C_3N][SO_4H].

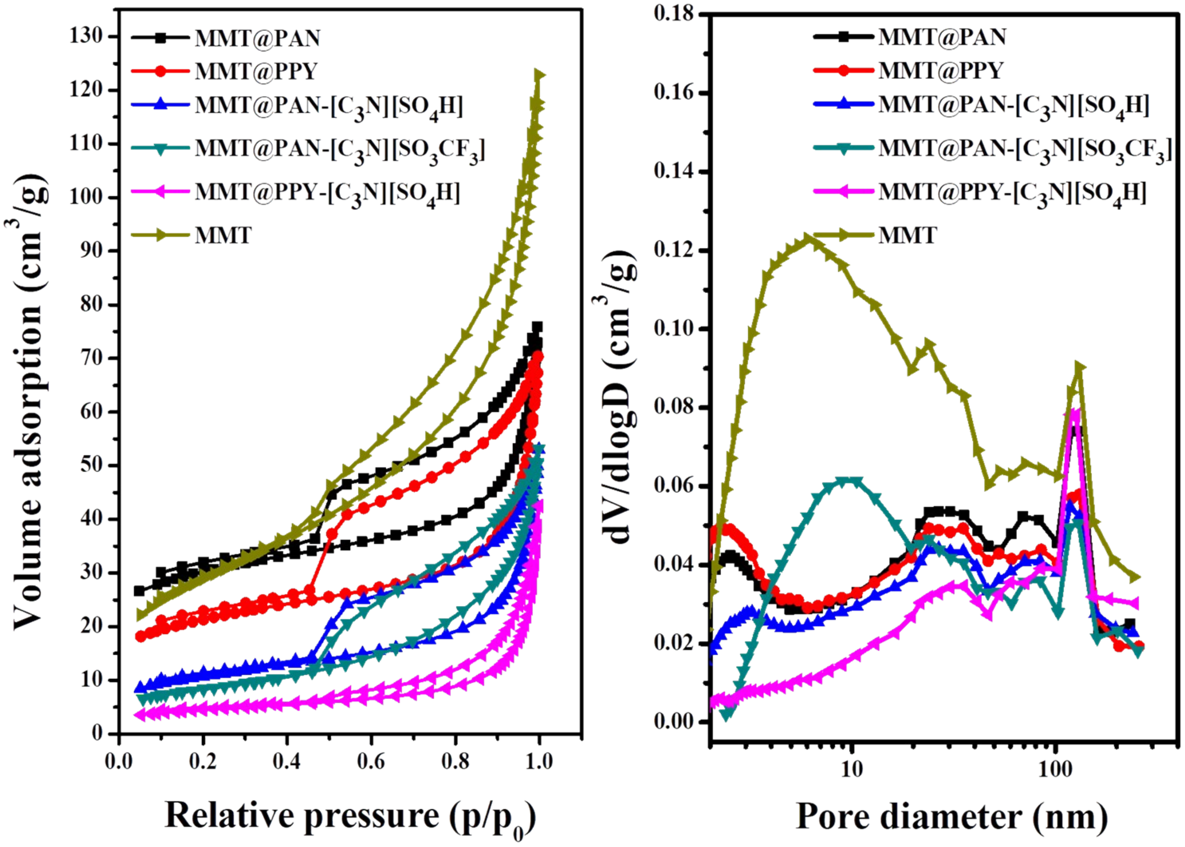

Figure S2 N_2 adsorption–desorption isotherms at -196 °C (left) and pore size distribution (right) of MMT, MMT@PAN, MMT@PPY, MMT@PAN-[C_3N][SO_3CF_3], MMT@PAN-[C_3N][SO_4H] and MMT@PPY-[C_3N][SO_4H].

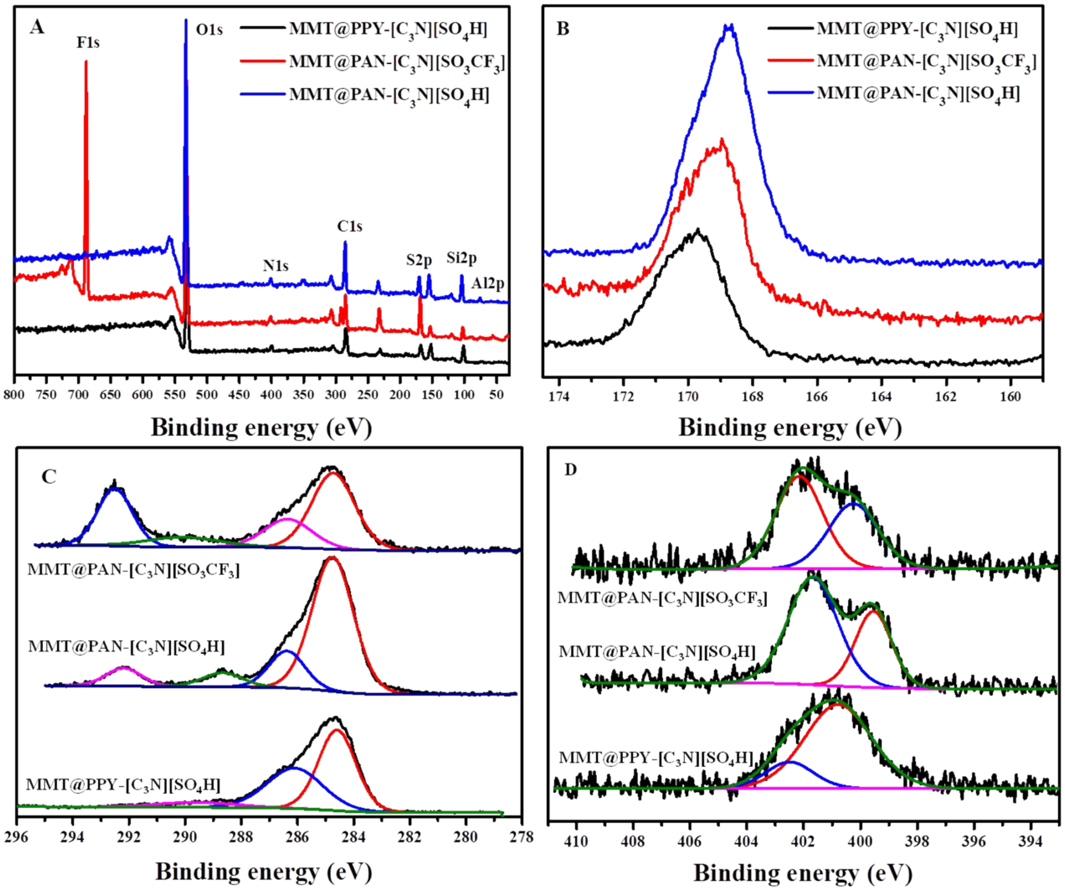

Figure S3 XPS spectra of (A) survey, (B) S_{2p}, (C) C_{1s} and (D) N_{1s} of the synthesized 2D solid acids.

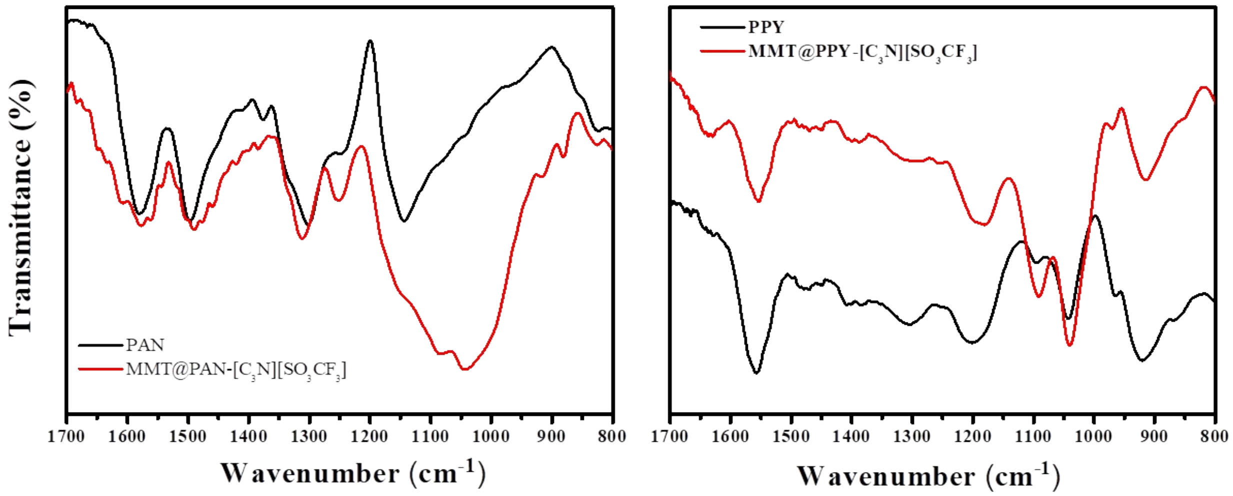

Figure S4 FT-IR spectra of PAN, MMT@PAN-[C_3N][SO_3CF_3], PPY and MMT@PPY-[C_3N][SO_3CF_3].

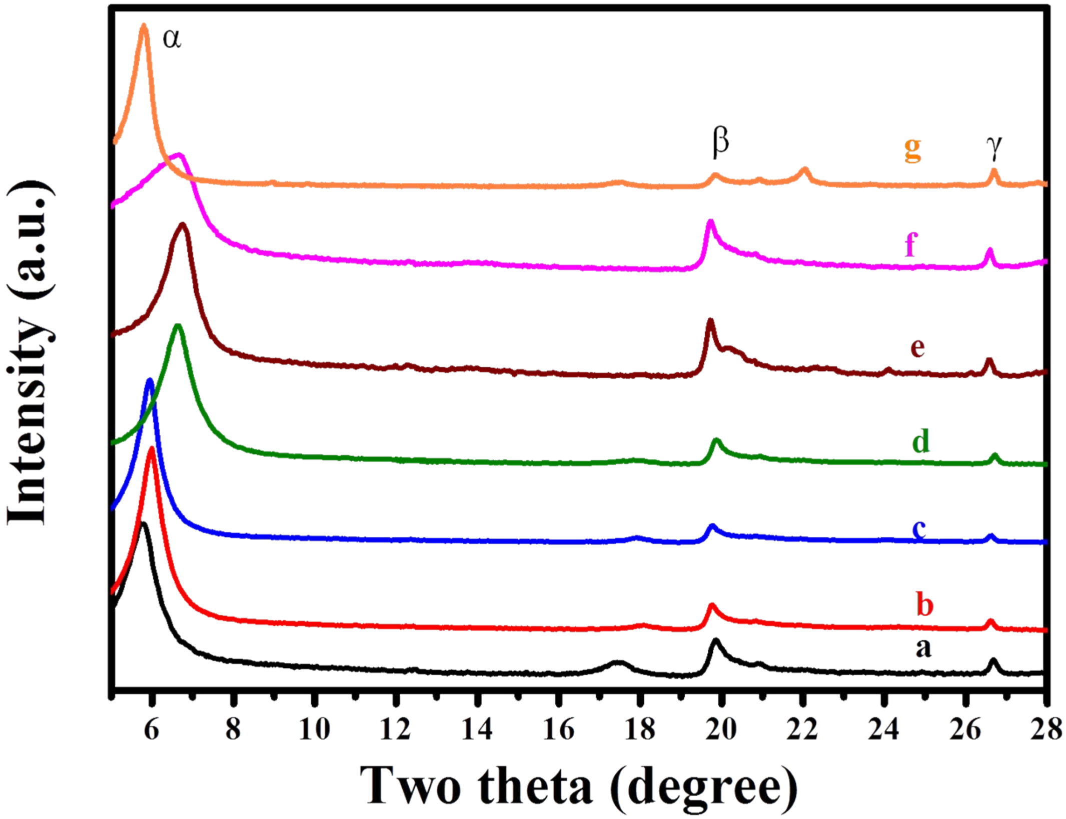

Figure S5 XRD patterns of (a) MMT, (b) MMT@PAN, (c) MMT@PPY, (d) MMT@PPY-[C_3N][SO_4H], (e) MMT@PAN-[C_3N][SO_4H], (f) MMT@PAN-[C_3N][SO_3CF_3] and (g) calcined MMT@PAN-[C_3N][SO_3CF_3] at 350 °C with flowing oxygen for removing of PAN-[C_3N][SO_3CF_3].

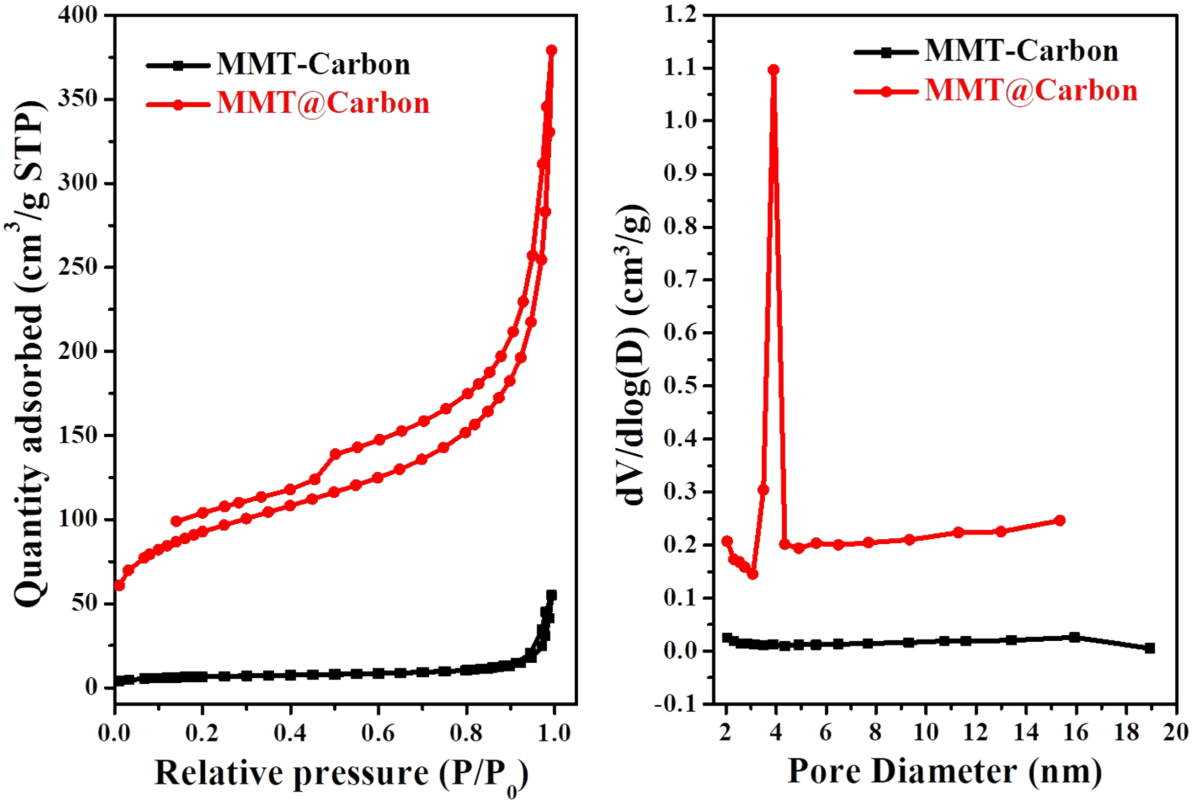

Figure S6 Compare the N_2 isotherms (Left) and pore size distribution (Right) of MMT-Carbon and MMT@Carbon.

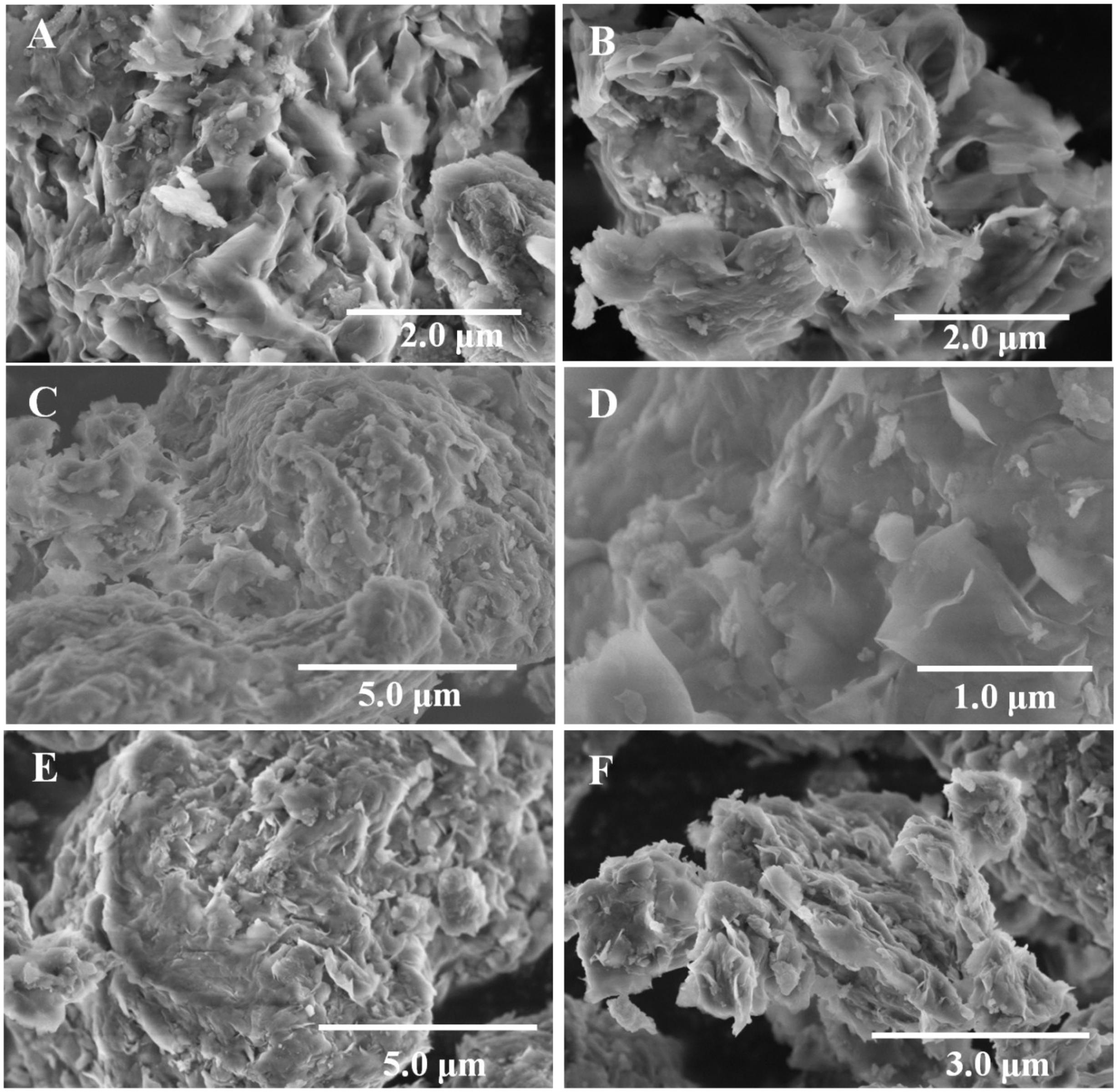

Figure S7 SEM images of (A, B) MMT, (C, D) MMT@PAN-[C_3N][SO_3CF_3] and (E, F) MMT@PPY-[C_3N][SO_3CF_3].

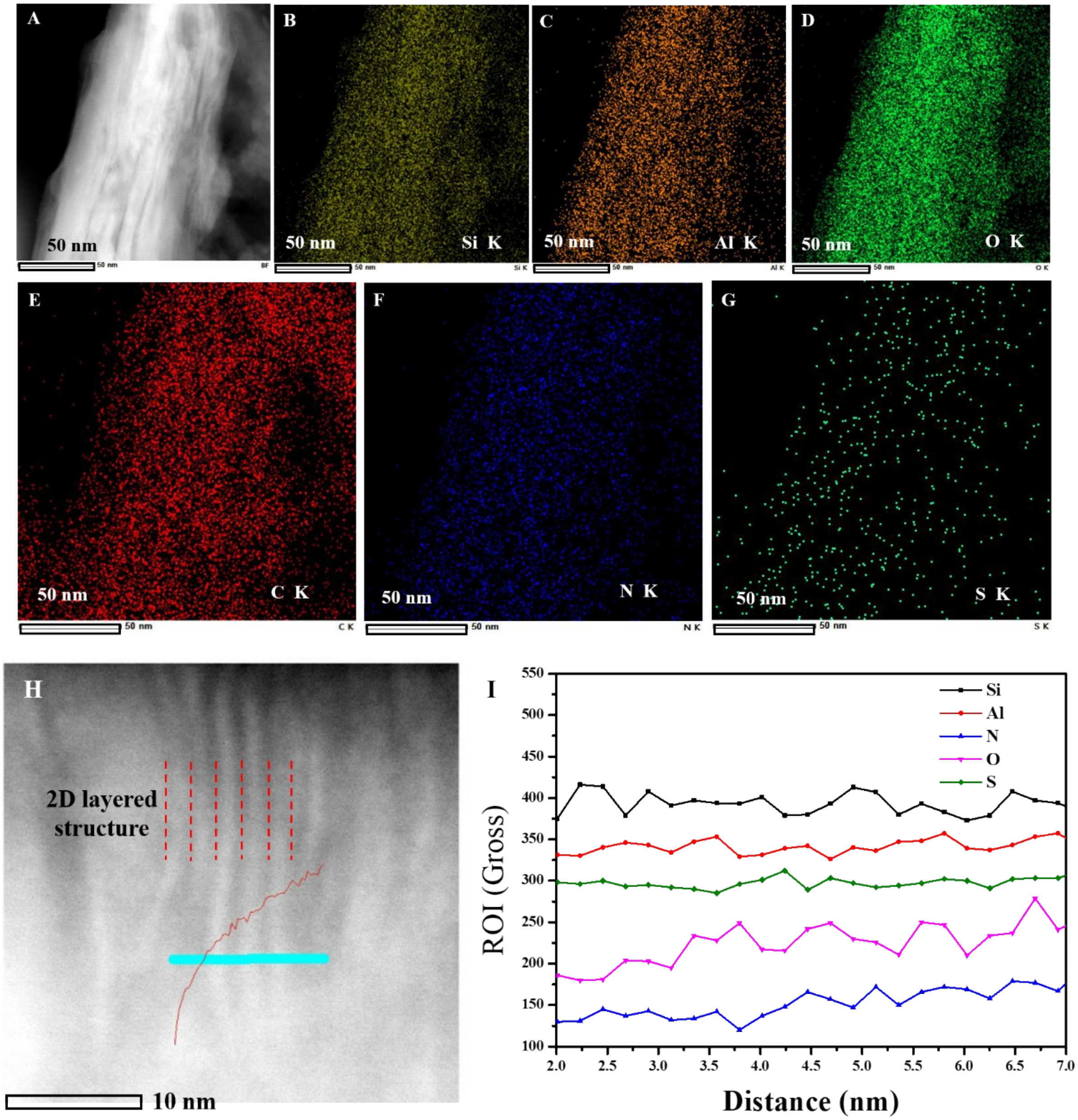

Figure S8 (A) STEM image and elemental maps of (B-G) Si, Al, O, C, N, S of MMT@PAN-[C_3N][SO_3CF_3], and (H&I) linear elements scanning of MMT@PAN-[C_3N][SO_3CF_3].

Diffusion Characterization and Molecular Dynamics Simulation

Molecular dynamics (MD) simulation was used to investigate the diffusion behavior of methanol and acetic acid molecules in zeolites and MMT. The detail of calculation diffusion coefficient (D_s) has been described in our previous work.[S15] As shown in Table S3, D_s of both methanol and acetic acid molecules in MMT were at least 1 order faster than that in zeolites, which shows less diffusion hinder of the guest in MMT (Table S3). The model and computational details are as follows.

The initial structures of zeolites were taken from the International Zeolite Associations database[S16] and followed super cell frameworks were chosen as 2 × 2 × 2, 2 × 2 × 5 and 2 × 2 × 5 for MFI (40.18 × 39.48 × 26.28 $Å^3$), MOR (36.51× 41.07 × 37.71 $Å^3$) and VFI (36.57 × 36.57 × 42.95 $Å^3$), respectively. While three layers of MMT (31.08 × 26.94 × 67.93 $Å^3$) were built based on the structures optimized by previous DFT calculation. The loading number of molecules in MFI, MOR, VFI zeolites and MMT were 27, 32, 28 and 30 per super cell, respectively. Initial structures with methanol and acetic acid molecules were shown in Figure S8 & S9.

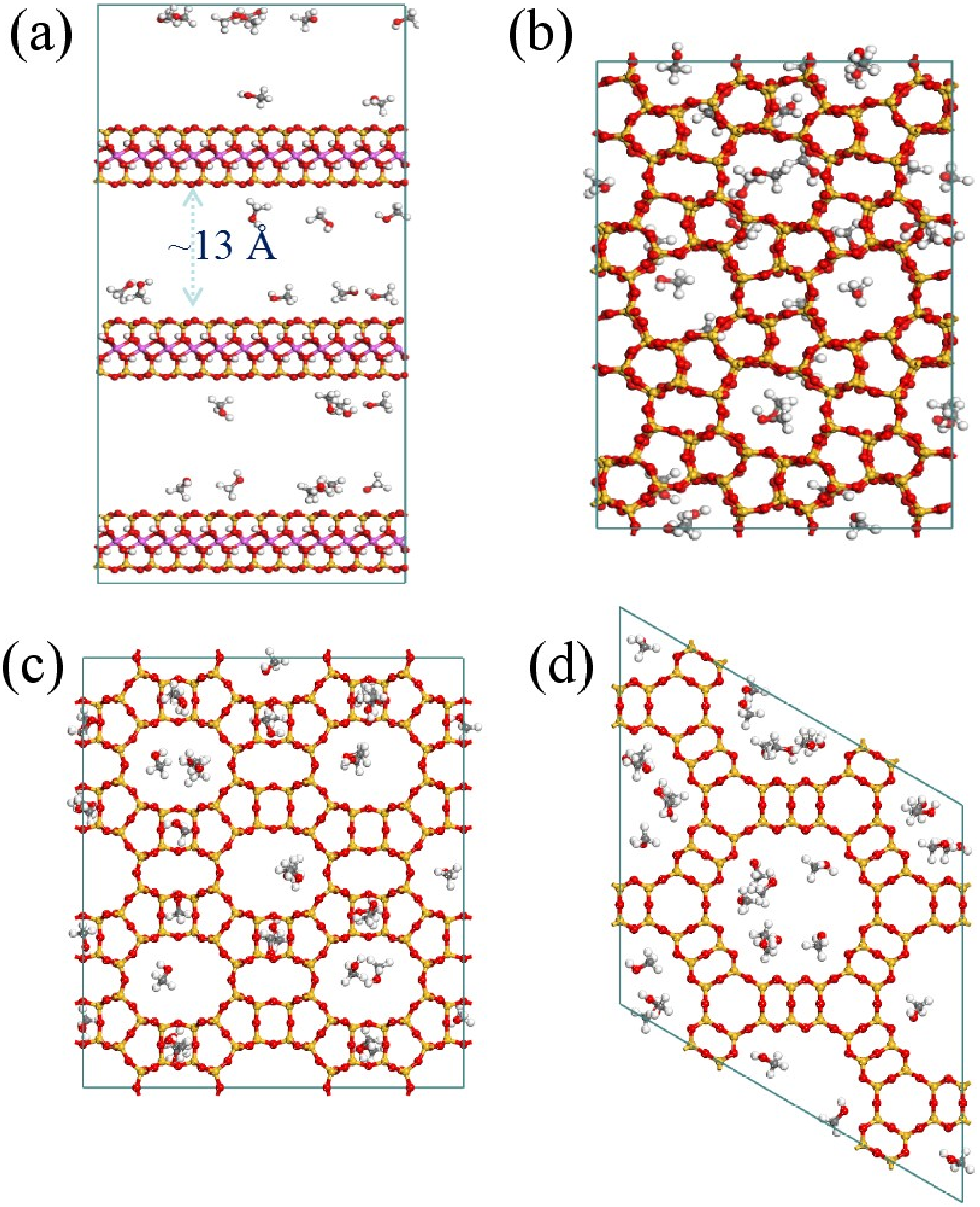

Figure S9 Initial atomic structure of methanol molecules adsorbed in (a) MMT along the [010] direction, (b) MFI along the [010] direction, (c) MOR along the [001] direction and (d) VFI along the [001] direction. Red, yellow, pink and white spheres represent oxygen, silicon, aluminum and hydrogen atoms, respectively.

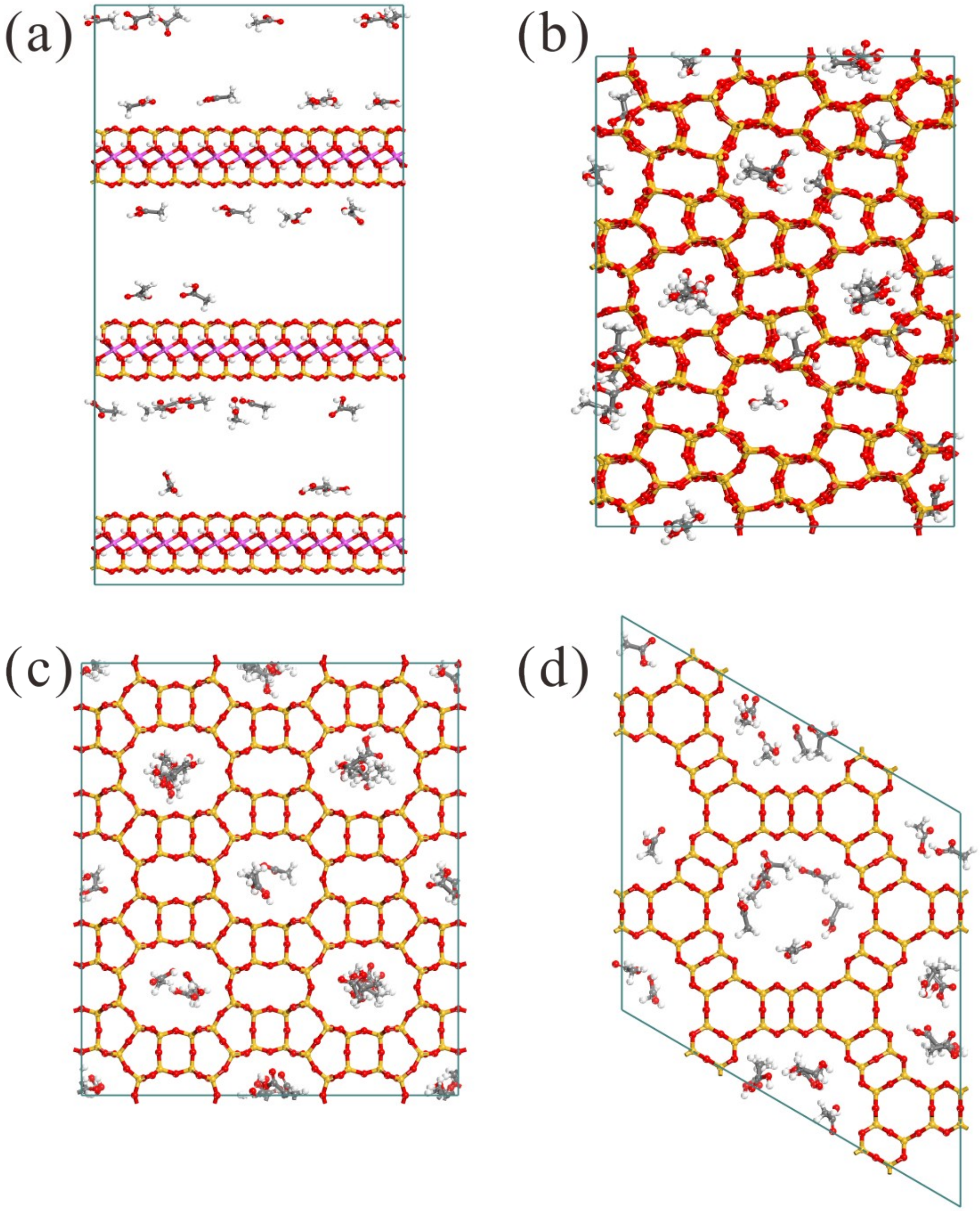

Figure S10 Initial atomic structure of acetic acid molecules adsorbed in (a) montmorillonite along the [010] direction, (b) MFI along the [010] direction, (c) MOR along the [001] direction and (d) VFI along the [001] direction. Red, yellow, pink and white spheres represent oxygen, silicon, aluminum and hydrogen atoms, respectively.

MD simulation was performed in the canonical ensemble (NVT), where the number of particles (N), simulation volume (V), and temperature (T) were kept constant. The simulated temperatures were 338 and 373 K for methanol and acetic acid in the catalytic reactions, respectively. During the simulation, the temperature was controlled by a Nosé-Hoover thermostat with a coupling time constant of 1 ps and the velocity Verlet algorithm was used to integrate the Newton's equations of motion with a time step of 1 fs. The force field parameters for the MMT and zeolites model were taken from the CLAYFF force field,[S17] which has been successfully applied to clay mineral system.[S18,S19] The OPLS force field was used to represent methanol and acetic acid molecules.[S20−S22] In the simulation, except for the rotation and stretching of hydrogen atoms, frameworks of MMT and zeolites were rigid. The interactions were described by Lennard-Jones (LJ) and Coulomb potential, and the LJ cross-interaction parameter were obtained by the Lorentz-Bertelot mixing rules ($\sigma_{ij} = (\sigma_{ii} + \sigma_{jj}) / 2$ and $\varepsilon_{ij} = (\varepsilon_{ii}\varepsilon_{jj})^{1/2}$). The long range electrostatic interactions were calculated using the Ewald summation method and LJ interactions were calculated with a 12 Å cutoff radius. Each MD simulation was equilibrated for 3 ns, then following 50 ns production for studying the diffusion behavior of guest molecules. The trajectories were recorded every 1000 steps and three MD simulations were carried out for better statistics. All MD were performed in the parallel general purpose DL_POLY_2.20 code.[S23]

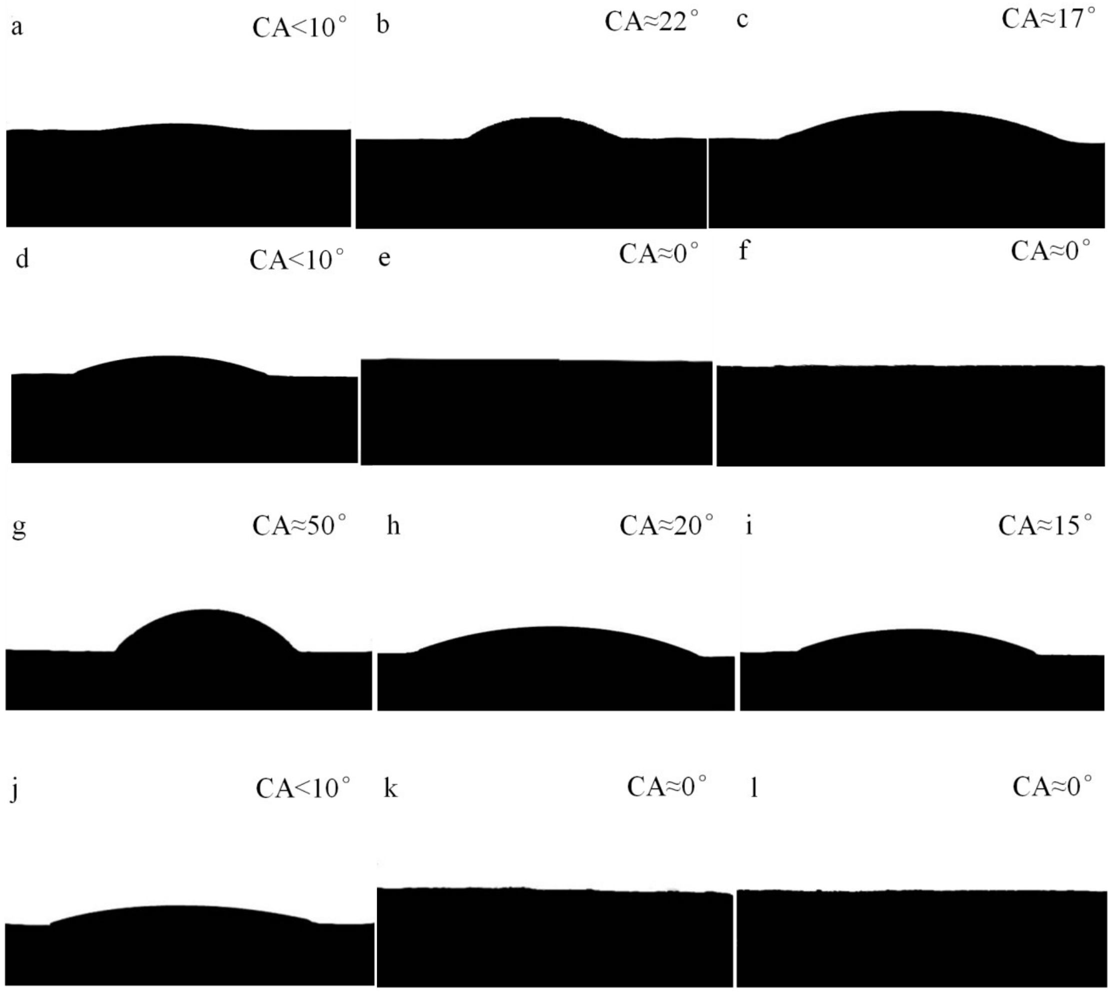

Figure S11 Contact angles of MMT and MMT@PAN-[C_3N][SO_3CF_3] for (a, g) water, (b, h) sunflower oil, (c, i) cyclohexanol, (d, j) acetic acid, (e, k) methanol and (f, l) toluene.

Figure S11 shows contact angles of MMT and MMT@PAN-[C_3N][SO_3CF_3] for water and various organic compounds, which was a reliable technique to investigate the surface wettability of various solid catalysts.[S24] MMT shows a contact angle for water lower than 10°, indicating its superhydrophilicity. After intercalation of PAN and sulfonation of the composites to give MMT@PAN-[C_3N][SO_3CF_3], which exhibits the contact angle for water at around 50°, indicating its certain hydropholicity. On the other hand, MMT@PAN-[C_3N][SO_3CF_3] shows the contact angle for sunflower oil at around 20°, indicating its very good oleophilic features, which could also be observed in that of MMT (22°). Moreover, MMT@PAN-[C_3N][SO_3CF_3] shows superwettability for various organic reactants. For instance, the contact angles of MMT@PAN-[C_3N][SO_3CF_3] for cyclohexanol, acetic acid, methanol and toluene was 15°, 10° <, 0° and 0° respectively. Similar superwettability for these reactants could also be observed in the MMT support. The above results confirm that both MMT and its derived 2D hybrid solid acids showed very good wettability for various reactants, which was favorable for the enhancement of compatibility of synthesized 2D solid acid in various chemical reactions. Good wettability and compatibility largely promote the fast diffusion of reactants into the inner channels of the synthesized 2D solid acid, which results in their enhanced mass transfer and good anti carbon deposition property.[S24]

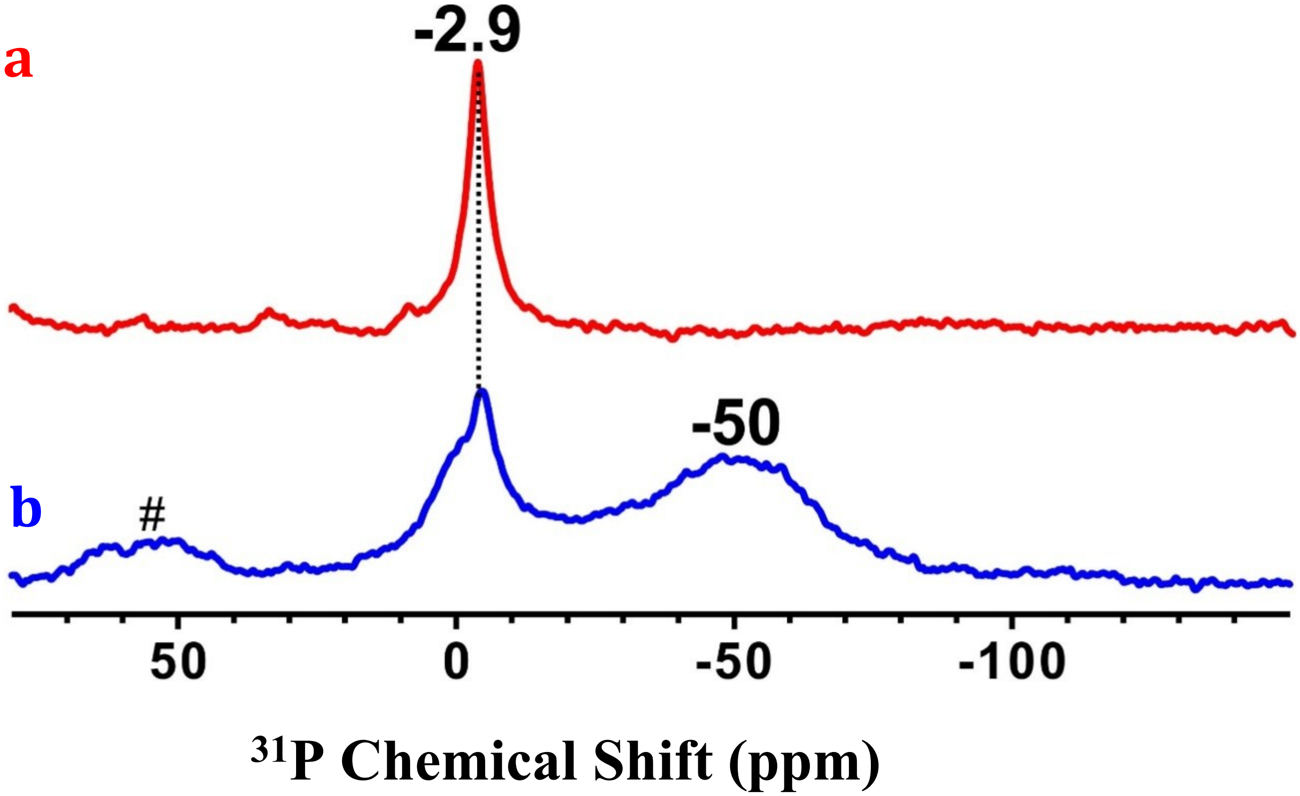

Figure S12 Room temperature ^{31}P MAS NMR spectra of trimethylphosphine (TMP) adsorbed on (a) MMT@PAN-[C_3N][SO_3CF_3] and (b) MMT.

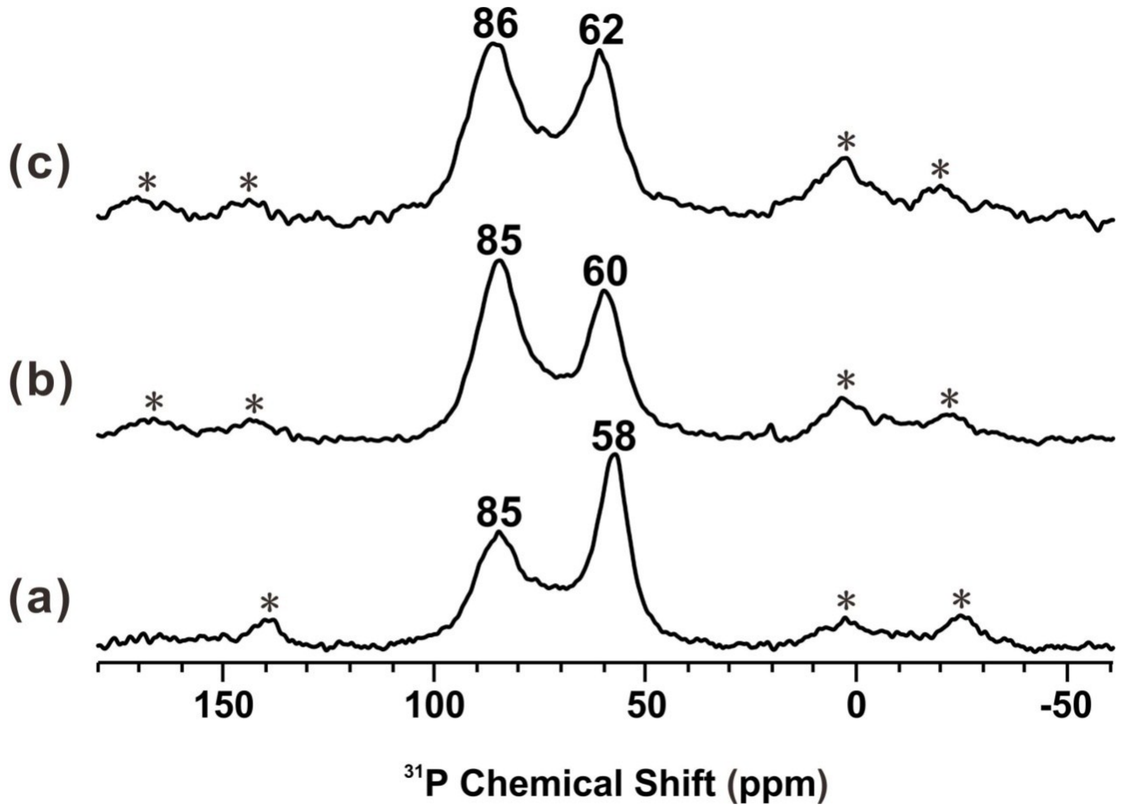

Figure S13 Room temperature ^{31}P MAS NMR spectra of trimethylphosphine (TMPO) adsorbed on (a) MMT@PAN-[C_3N][SO_4H]-0.2, (b) MMT@PAN-[C_3N][SO_4H]-0.4 and (c) MMT@PPY-[C_3N][SO_3CF_3]. The asterisks in the ^{31}P NMR spectra denote spinning sidebands.

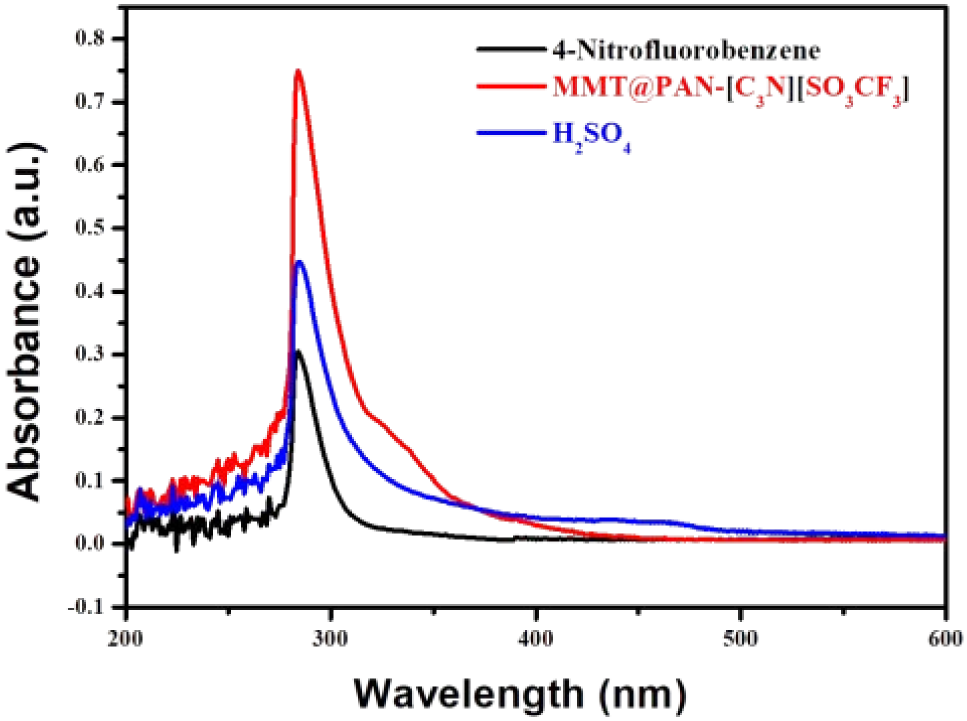

Figure S14 UV-spectra of 4-nitrofluorobenzene solution interacted with H_2SO_4 and MMT@PAN-[C_3N][SO_3CF_3].

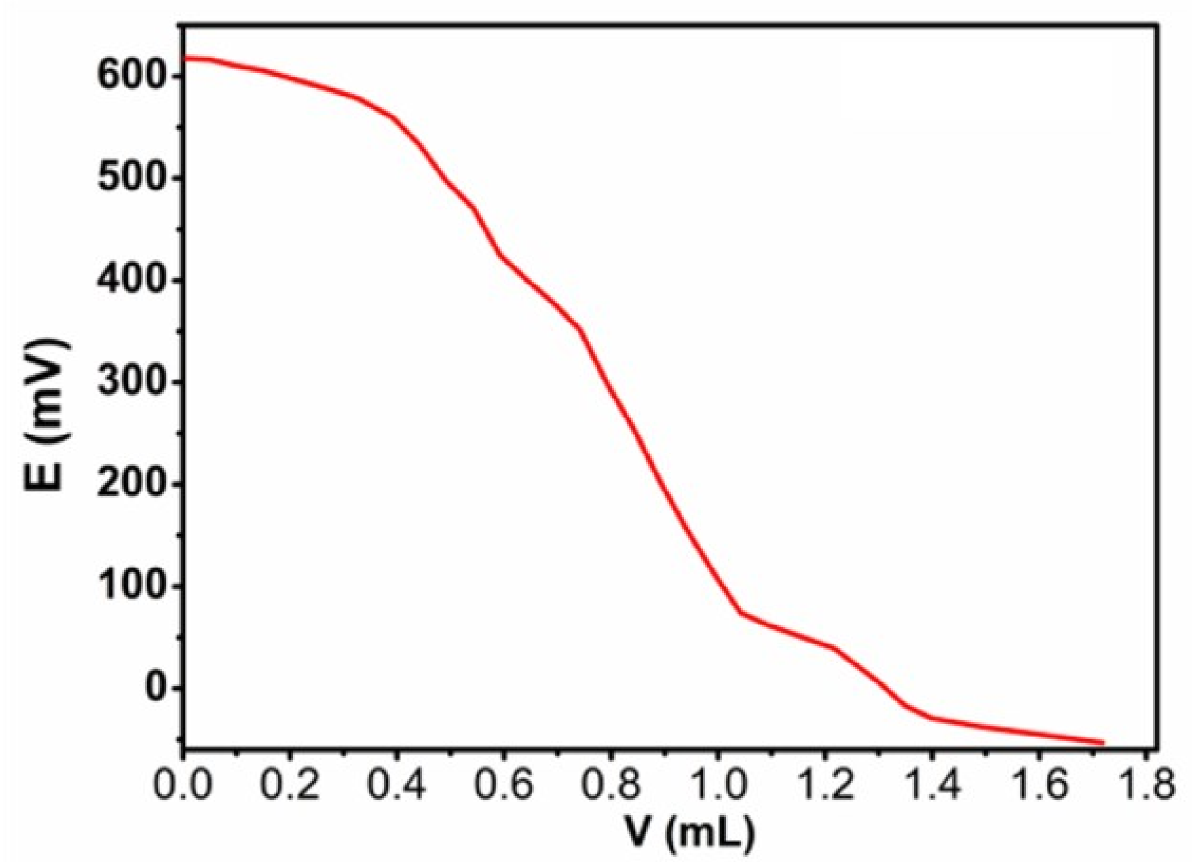

Figure S15 Potentiometric titration curve of MMT@PAN-[C_3N][SO_3CF_3].

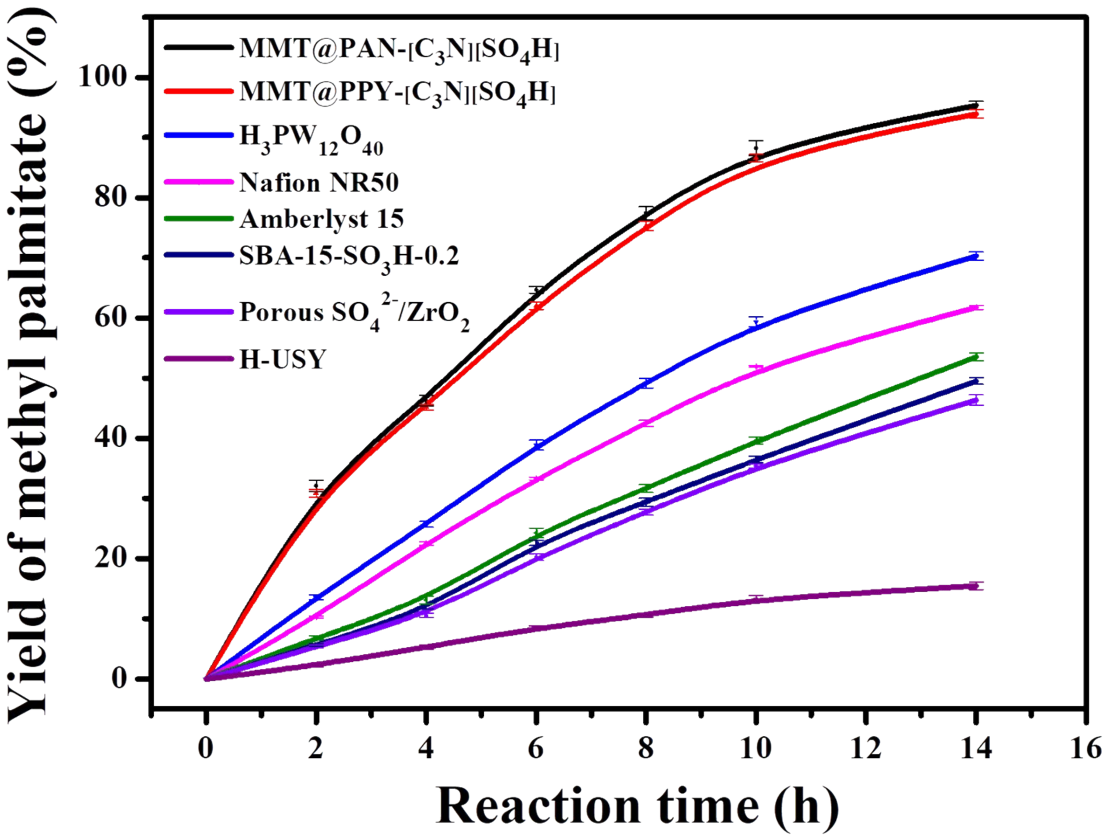

Figure S16 Yields of methyl palmitate catalyzed of various acid catalysts in transesterification of tripalmitin with methanol.

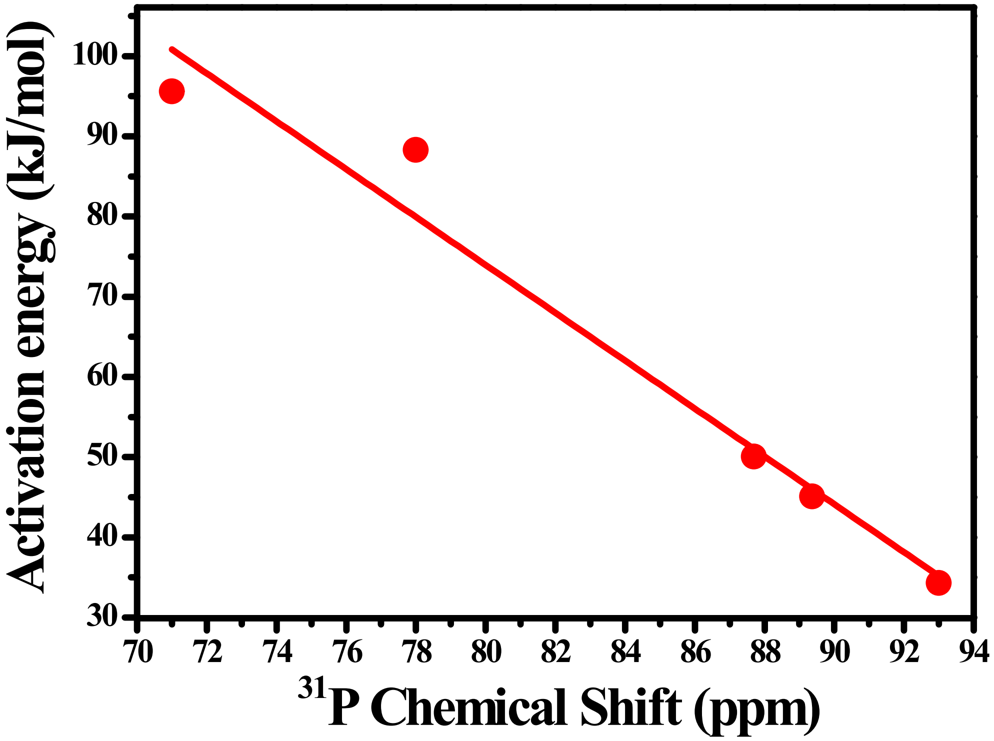

Figure S17 Relationship between activation energy and acid strength evaluated from ^{31}P chemical shifts of MMT@PAN-[C_3N][SO_3CF_3], H_2SO_4, $H_3PW_{12}O_{40}$, Amberlyst-15 and SBA-15-SO_3H-0.2 in the transesterification of tripalmitin with methanol.

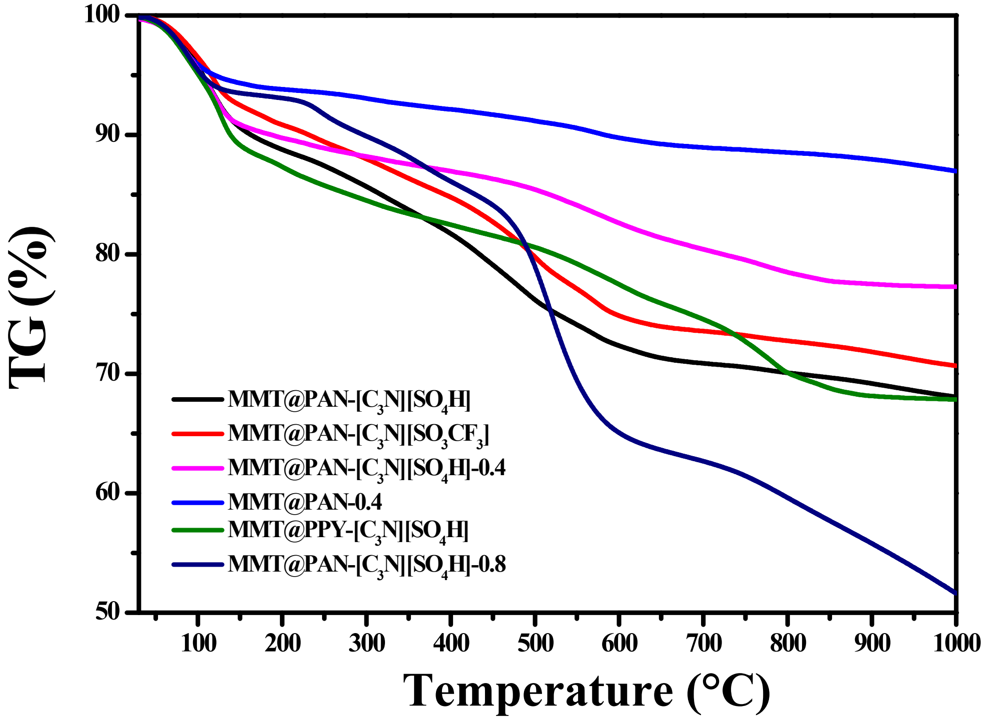

Figure S18 TG curves of various synthesized 2D hybrid solid acids.

Figure S18 shows the TG curves of the synthesized 2D hybrid solid acids. The weight loss in the temperature range of 50–150 °C should be attributed to desorption of the absorbed water in the samples. The 2D hybrid solid acids exhibit similar decomposition behaviors, with significant weight loss in the temperature range of 450–600 °C as a result of the destruction of sulfonate group and polymeric networks. The residual weights (higher than 52%) could be observed in all samples even when the combustion temperature increased up to 1000 °C, which should be attributed to the residual MMT support. The high decomposition temperatures verify very good thermal stability of the 2D hybrid solid acids, which should be attributed to high molecular weight of polymeric layer and unique inorganic-organic hybrid nanostructures.

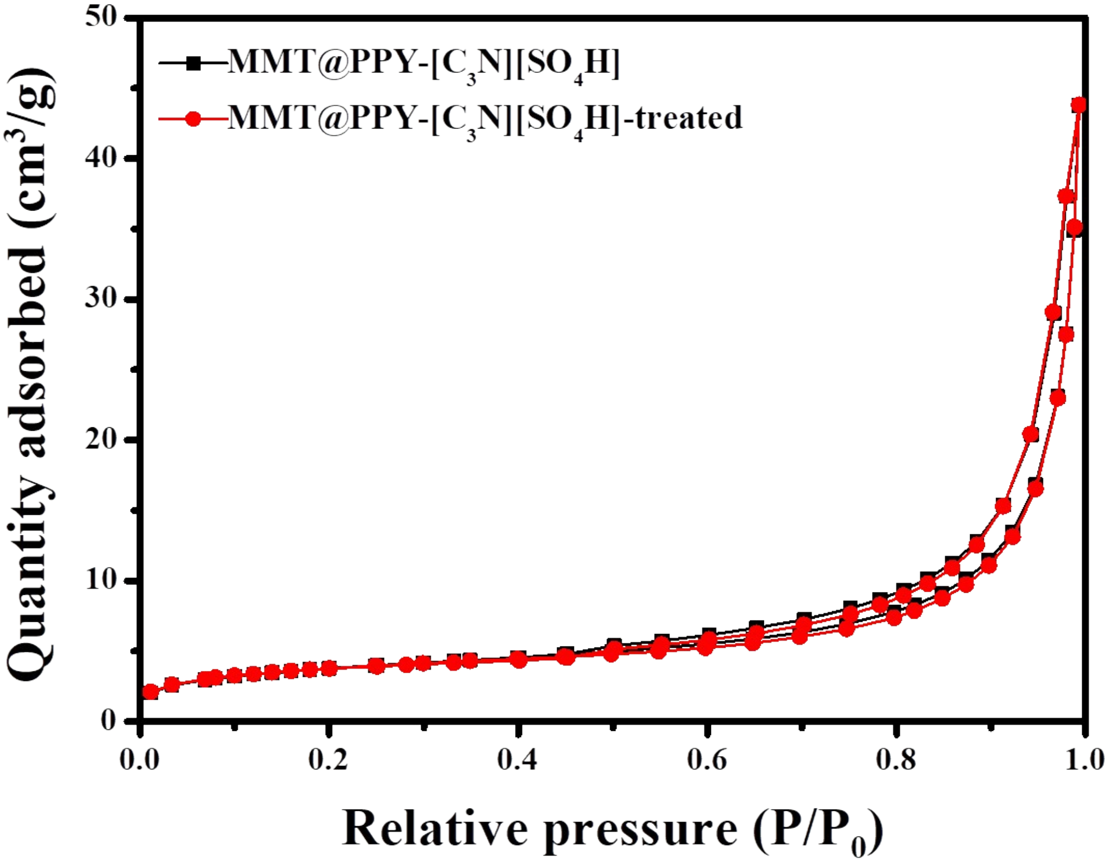

Figure S19 N_2 isotherms of MMT@PPY-[C_3N][SO_4H] before (black) and after (red) hydrothermal treatment at 200 °C for 4 h.

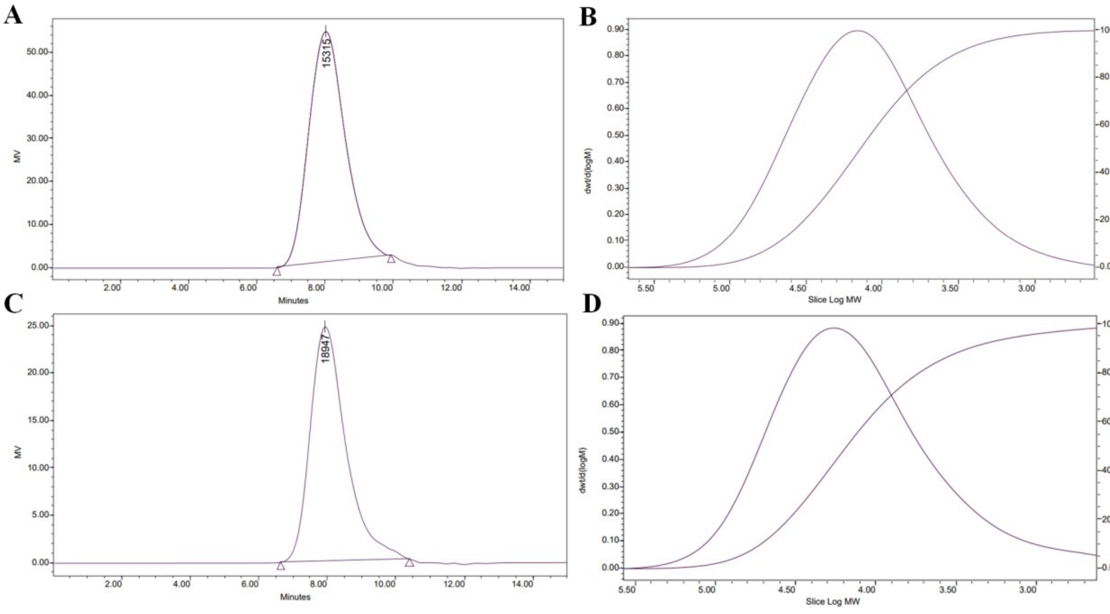

Figure S20 Gel permeation chromatography (GPC) spectra and molecular weight distribution curve of (A,B) PAN-[C_3N][SO_3CF_3] and (C,D) PPY-[C_3N][SO_4H].

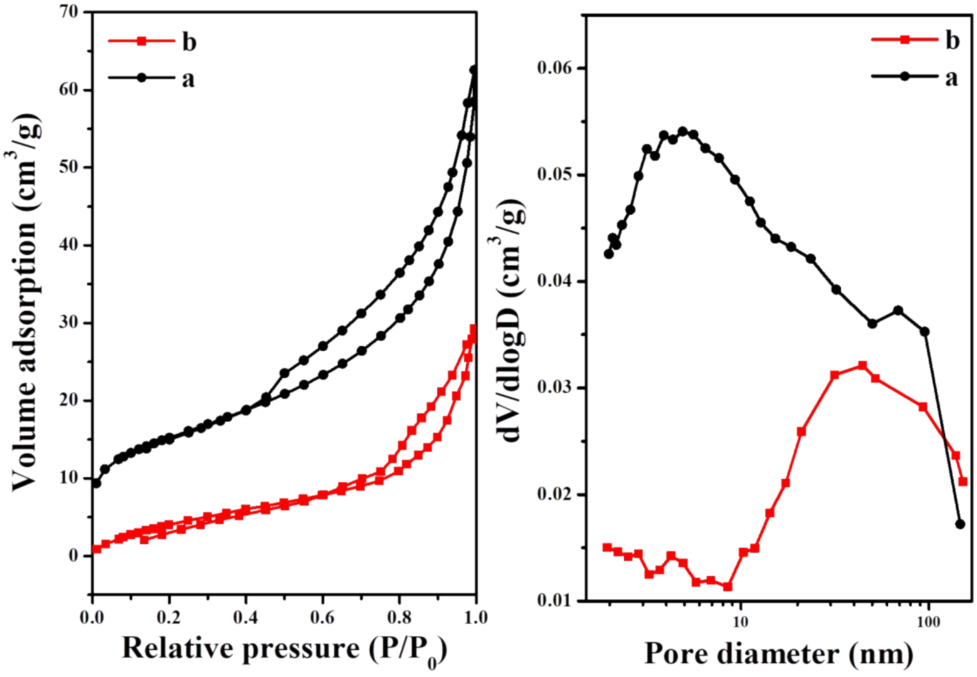

Figure S21 N_2 isotherms and pore size distribution of MMT@PAN-[C_3N][SO_4H]-0.4 (a) before and (b) after adsorption of crystalline cellulose of Avicel.

Figure S21 shows N_2 isotherms and pore size distribution of MMT@PAN-[C_3N][SO_4H]-0.4 before and after adsorption of crystalline cellulose of Avicel. Compared with MMT@PAN-[C_3N][SO_4H]-0.4, a decreasing of volume adsorption was observed after the adsorption of crystalline cellulose (Figure S21). More interestingly, obvious changes in the pore size distribution can be observed after introduction of crystalline cellulose into MMT@PAN-[C_3N][SO_4H]-0.4. For example, the macropore size decreased from 67.5 nm to 43.5 nm, and mesopore size distribution at around 5.1 nm were basically disappeared, which indicates fully blocking of mesopores by crystalline cellulose. The above results confirm that the structural defects and locally distorted structures in the synthesized 2D solid acids were large enough for the crystalline cellulose macromolecules to diffuse in and out.

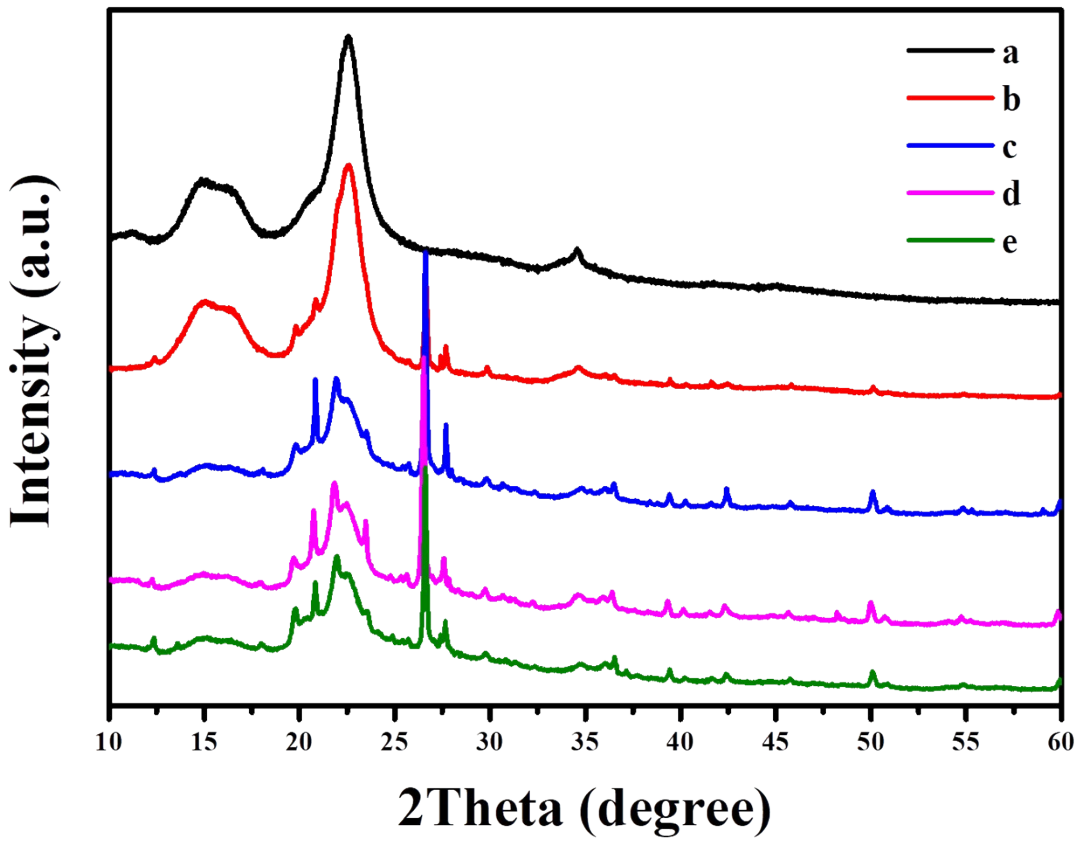

Figure S22 XRD patterns of (a) crystalline cellulose of Avicel, and the Avicel being treated by MMT@PAN-[C_3N][SO_3CF_3] at 100 °C for (b) 0 h, (c) 2 h, (d) 3 h and (e) 5 h.

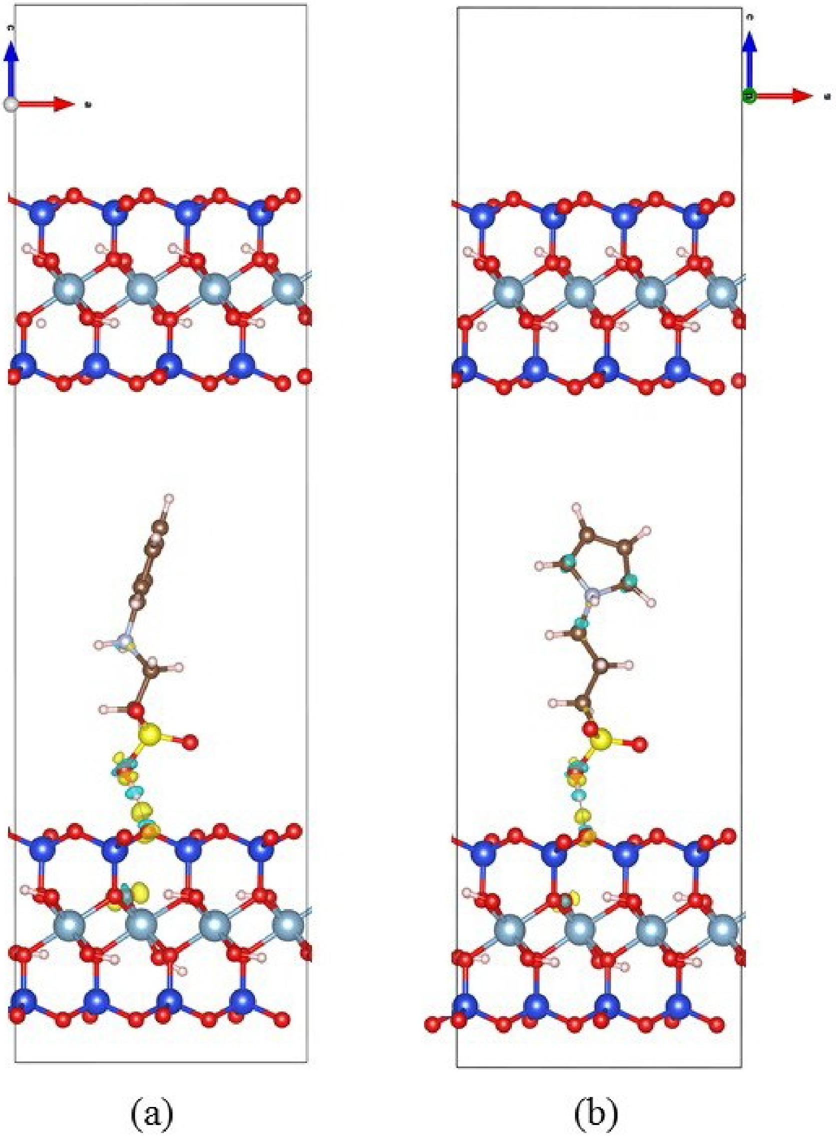

(a) (b)

Figure S23 The deformation charge density graphic of (a) sulfonated aniline and (b) sulfonated aniline and pyrrole monomer in the internal layer of MMT support (iso$_{\text{value}}$ = 0.01 a.u.).

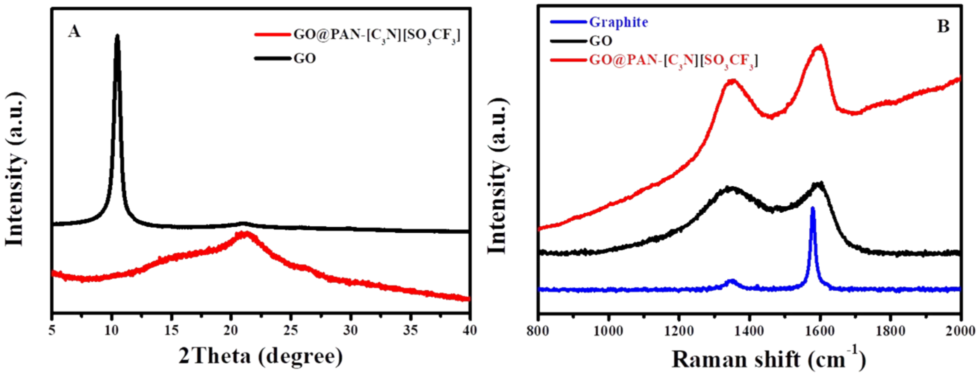

Figure S24 (A) XRD patterns and (B) Raman spectra of graphite, graphitic oxide (GO) and GO@PAN-[C_3N][SO_3CF_3].

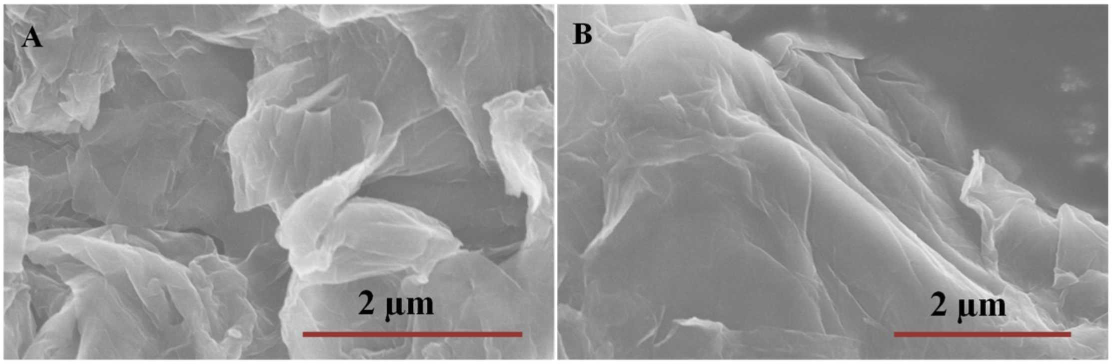

Figure S25 SEM images of GO and GO@PAN-[C_3N][SO_3CF_3].

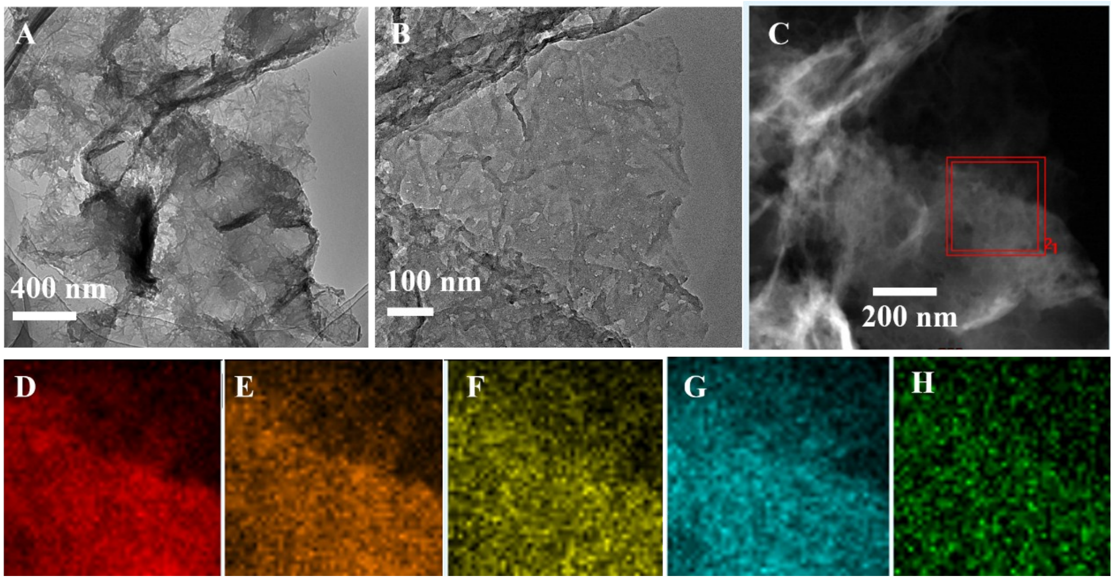

Figure S26 (A&B) TEM images, (C) STEM image and (D-H) elemental maps of C, N, O, S, F, of GO@PAN-[C_3N][SO_3CF_3].

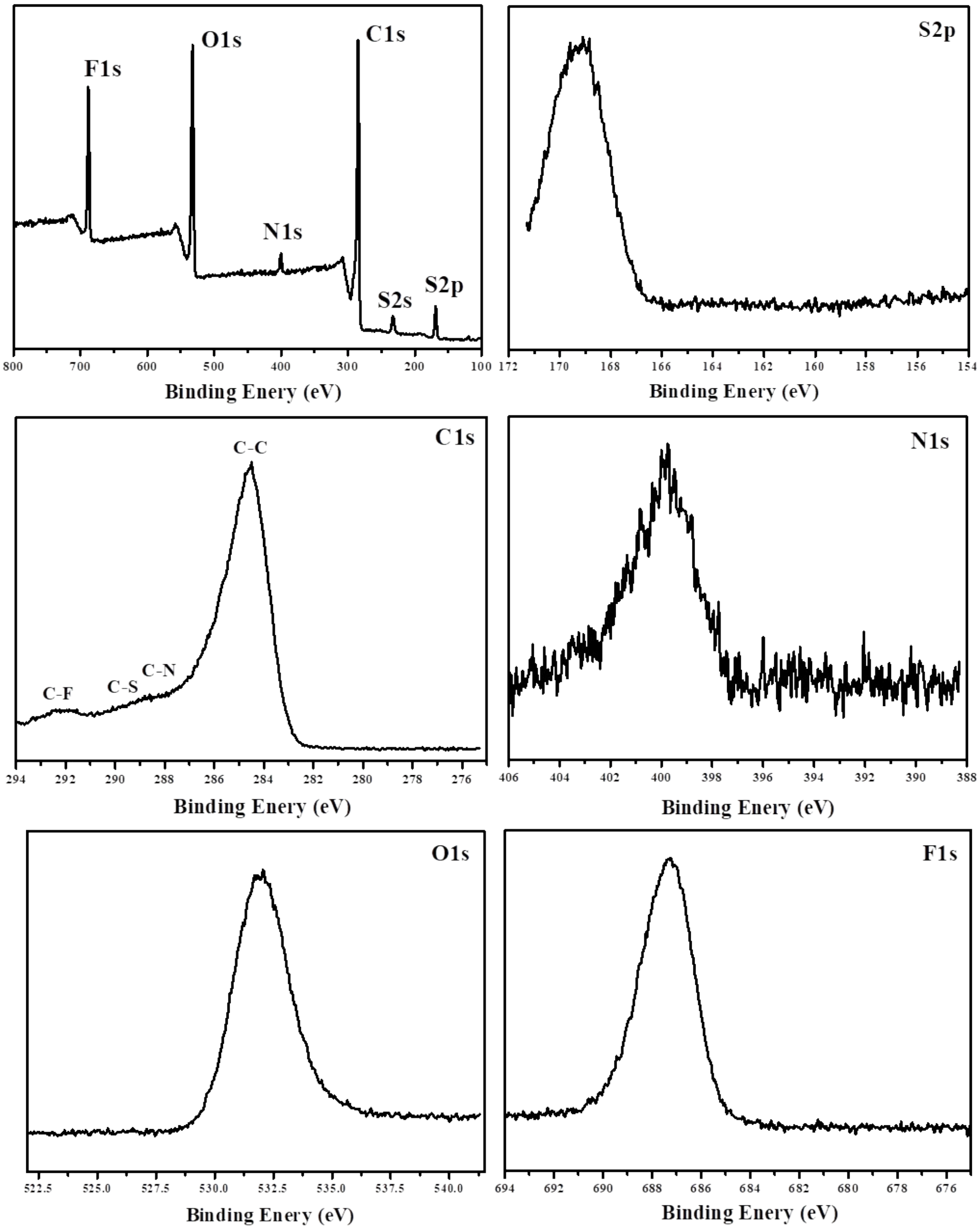

Figure S27 XPS spectra of GO@PAN-[C_3N][SO_3CF_3].

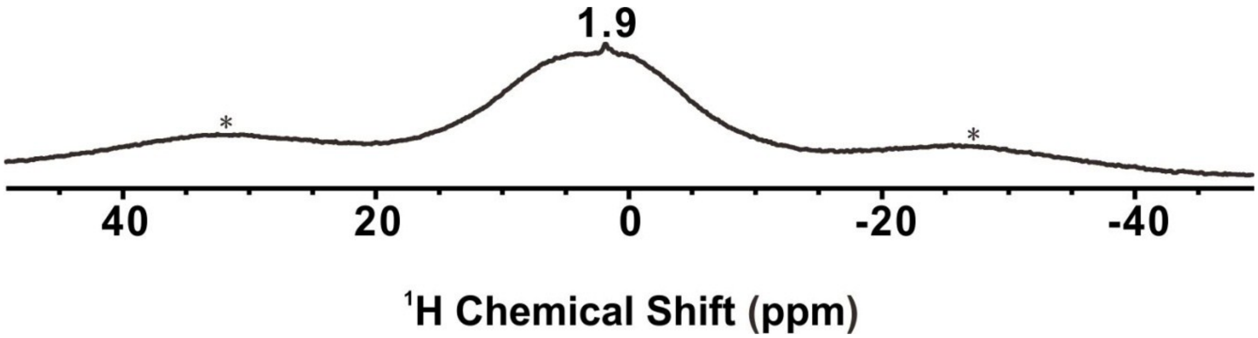

Figure S28 ^{1}H solid-state NMR spectra of GO@PAN-[C_3N][SO_3CF_3].

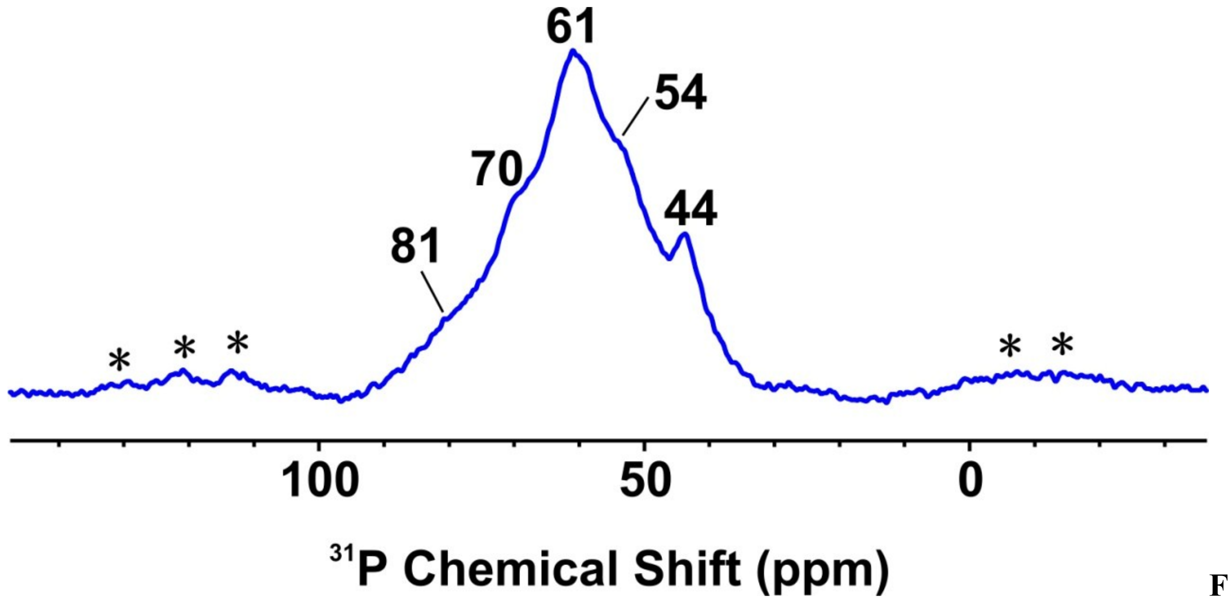

F

igure S29 (A) Room temperature ^{31}P MAS NMR spectra of trimethylphosphine (TMPO) adsorbed on GO@PAN-[C_3N][SO_3CF_3].

Supporting references

S1. W. S. Hummers Jr and R. E. Offeman, *J. Am. Chem. Soc.*, 1958, **80**, 1339.

S2. D. Margolese, J. A. Melero, S. C. Christiansen, B. F. Chmelka and G. D. Stucky, *Chem. Mater.*, 2000, **12**, 2448−2459.

S3. Y. Y. Sun, L. Zhu, H. J. Lu, R. W. Wang, S. Lin, D. Z. Jiang and F.-S. Xiao, *Appl. Catal. A-Gen.*, 2002, **237**, 21−31.

S4. A. M. Zheng, H. L. Zhang, X. Lu, S.-B. Liu and F. Deng, *J. Phys. Chem. B*, 2008, **112**, 4496−4505.

S5. A. M. Zheng, S. J. Huang, S.-B. Liu and F. Deng, *Phys. Chem. Chem. Phys.*, 2011, **13**, 14889−14901.

S6. N. Feng, A. M. Zheng, S.-J. Huang, H. L. Zhang, N. Y. Yu, C.-Y. Yang, S.-B. Liu and F. Deng, *J. Phys. Chem. C*, 2010, **114**, 15464−15472.

S7. T. Nakahira, L. Fan, C. T. Boon, T. Fukada, T. Karato, M. Annaka and M. Yoshikuni, *Polymer J.*, 1998, **30**, 910−914.

S8. J. P. Perdew, K. Burke and M. Ernzerhof, *Phys. Rev. Lett.*, 1996, **77**, 3865–3868.

S9. B. Delley, *J. Chem. Phys.*, 1990, **92**, 508–517.

S10. B. Delley, *J. Chem. Phys.*, 2000, **113**, 7756–7764.

S11. S. Grimme, *J. Comput. Chem.*, 2006, **27**, 1787–1799.

S12. K. Momma and F. Izumi, *J. Appl. Crystallogr.*, 2011, **44**, 1272–1276.

S13. R. Rinaldi, R. Palkovits, F. Schüth, *Angew. Chem., Int. Ed.*, 2008, **47**, 8047–8050.

S14. F. J. Liu, R. K. Kamat, I. Noshadi, D. Peck, R. S. Parnas, A. M. Zheng, C. Z. Qi and Y. Lin, *Chem. Commun.*, 2013, **49**, 8456−8458.

S15. Z. Q. Liu, Y. Y. Chu, X. M. Tang, L. Huang, G. C. Li, X. F. Yi and A. M. Zheng, *J. Phys. Chem. C*, 2017, **121**, 22872−22882.

S16. C. Baerlocher and L. B. McCusker, Database of Zeolite Structures: http://www.iza-structure.org/databases/.

S17. R. T. Cygan, J. J. Liang and A. G. Kalinichev, *J. Phys. Chem. B*, 2004, **108**, 1255–1266.

S18. J. A. Greathouse, D. B. Hart, G. M. Bowers, R. J. Kirkpatrick and R. T. Cygan, *J. Phys. Chem. C*, 2015, **119**, 17126−17136.

S19. J. Shi, Z. Y. Lou, M. L. Yang, Y. Zhang, H. B. Liu and Y. F. Meng, *Comput. Mater. Sci.*, 2015, **96**, 134−139.

S20. W. L. Jorgense, *J. Phys. Chem.*, 1986, **90**, 1276−1284.

S21. D. Gonzalez-Salgado and C. Vega, *J. Chem. Phys.*, 2016, **145**, 034508.

S22. S. Fathi, S. Bouazizi, S. Trabelsi, A. M. Gonzalez, M. Bahri, S. Nasr and M.-C. Bellissent-Funel, *J. Mol. Liq.*, 2014, **196**, 69−76.

S23. W. Smith and T. R. Forester, *J. Mol. Graphics.*, 1996, **14**, 136−141.

S24. L. Wang and F.-S. Xiao, *Green Chem.*, 2015, **17**, 24−39.